MPP-2014-548

Complete Intersection Fibers in F-Theory

Volker Braun,[1] Thomas W. Grimm,[2] and Jan Keitel[2]

[1]Mathematical Institute, University of Oxford
24-29 St Giles', Oxford, OX1 3LB, United Kingdom

[2]Max-Planck-Institut für Physik,
Föhringer Ring 6, 80805 Munich, Germany

arXiv:1411.2615v2 [hep-th] 28 Jan 2015

ABSTRACT

Global F-theory compactifications whose fibers are realized as complete intersections form a richer set of models than just hypersurfaces. The detailed study of the physics associated with such geometries depends crucially on being able to put the elliptic fiber into Weierstrass form. While such a transformation is always guaranteed to exist, its explicit form is only known in a few special cases. We present a general algorithm for computing the Weierstrass form of elliptic curves defined as complete intersections of different codimensions and use it to solve all cases of complete intersections of two equations in an ambient toric variety. Using this result, we determine the toric Mordell-Weil groups of all 3134 nef partitions obtained from the 4319 three-dimensional reflexive polytopes and find new groups that do not exist for toric hypersurfaces. As an application, we construct several models that cannot be realized as toric hypersurfaces, such as the first toric $SU(5)$ GUT model in the literature with distinctly charged **10** representations and an F-theory model with discrete gauge group $\mathbb{Z}_4$ whose dual fiber has a Mordell-Weil group with $\mathbb{Z}_4$ torsion.

November 12, 2014

volker.braun@maths.ox.ac.uk; grimm, jkeitel@mpp.mpg.de

Contents

1 Introduction **2**

2 Koszul and Residues **3**

3 Weierstrass Form for Complete Intersections **5**

3.1 Basic Algorithm 5

3.2 Sections of Line Bundles 7

3.3 The Second Differential 7

3.4 An Algorithm to Compute Relations 9

3.5 Kodaira Map 10

3.6 Two Exceptions 10

4 Classifying Toric Mordell-Weil Groups **12**

4.1 Complete Intersections in Toric Varieties 12

4.2 Nef Partitions of 3d Lattice Polytopes 13

4.3 Toric Mordell-Weil Groups 15

4.4 Results for Elliptic Curves of Codimension Two 17

5 Examples **21**

5.1 $SU(5) \times U(1)^2$ with Different Antisymmetric Representations 22

5.2 $SU(5) \times U(1)^2$ and a Discrete Symmetry 26

5.3 Example with Mordell-Weil Torsion $\mathbb{Z}_4$ 29

6 Conclusions **31**

A List of Non-Toric Non-Abelian Gauge Groups **32**

1 Introduction

F-theory [1] provides a convenient way of realizing the $SL(2,\mathbb{Z})$ symmetry of Type IIB string theory geometrically by relating it to the modular group acting on the complex structure of a T^2. In particular, the complex structure of this auxiliary two-torus is identified with the axio-dilaton of the low-energy effective action. For Calabi-Yau manifolds that are non-trivial T^2-fibrations one thus obtains a geometric description of a Type IIB background with varying axio-dilaton τ.

Since the axio-dilaton diverges at the position of D7-branes in the Type IIB compactification, τ contains information about the low-energy effective theory and is therefore one of the main quantities of interest. τ and especially the locus of its singularities can easily be obtained if the defining equation of the T^2 is given in Weierstrass form

$$y^2 = x^3 + fx + g\,. \tag{1.1}$$

In general, for every torus fibration with a global section a map into this form is guaranteed to exist. If the fibration does not have a global section, then one can replace the genus-one curve by its Jacobian, which is then guaranteed to have a section while maintaining the same discriminant.[1] In practice, however, finding this map can be challenging and the solution to this problem is only known in a few special cases. The simplest of these cases is the elliptic curve inside $\mathbb{P}_{231}$ whose generic form is given by

$$y^2 + a_1xyz + a_3yz^3 = x^3 + a_2x^2z^2 + a_4xz^6 + a_6z^6\,. \tag{1.2}$$

Equation (1.2) can be brought into Weierstrass form simply by completing the square and the cube with respect to y^2 and x^3. Possibly for this reason, much of the early F-theory literature focused on such scenarios and constructed Calabi-Yau manifolds inside $\mathbb{P}_{231}$ fibrations over B', with the T^2 a hypersurface in $\mathbb{P}_{231}$ and the base B_{n-1} a complete intersection in B'. In order to harness the full power of algebraic geometry, one ordinarily considers complete intersections whose defining equations have generic coefficients inside such a space. As soon as one does so, however, considering only fibers embedded in $\mathbb{P}_{231}$ heavily restricts the low-energy effective physics of the corresponding F-theory compactifications. In particular, generic fibers inside $\mathbb{P}_{231}$ do not lead to Abelian gauge factors. In recent years, the original focus on engineering non-Abelian gauge theories in global F-theory [3–5] has shifted towards advancing the understanding of their Abelian counterparts. As a consequence, it has become necessary to consider more general fiber embeddings, starting with a blow-up of $\mathbb{P}_{231}$ in [6], extended to more general cases with a single $U(1)$ in [7–10] and finally progressing to higher-rank $U(1)$s [11–15] and a treatment of embeddings in all 16 toric surfaces in [16, 17]. Most recently, torus fibers that do not generically have a section, i.e. genus-one curves that are not elliptic curves, have started to be investigated in [2, 17–22]. Furthermore, progress has been made in also understanding geometrically massive $U(1)$s [23, 24].

[1] However, the Jacobian might have terminal singularities even if the original fibration was smooth [2].

With the exception of [15], in which purely Abelian $U(1)^3$ models were studied, and [25] where an $SU(5)$ singularity was resolved using a complete intersection, all of these works have embedded the elliptic fiber as a *hypersurface* in a two-dimensional toric variety. For these cases, computing the Weierstrass form was developed in [26]. However, as shown in [16], this still imposes a considerable constraint on the resulting F-theory models. Apart from limiting the toric Mordell-Weil group to rank ≤ 3, the fact that the elliptic curve is a hypersurface in an ambient variety also restricts the possible resolutions of non-Abelian singularities. In particular, with respect to $SU(5)$ GUTs, it implies that there exists only a single antisymmetric matter representation in the spectrum of the low-energy effective theory. The restriction on the matter content applies of course only to *resolved* manifolds — after blowing down, singular models can be constructed as hypersurfaces, as is obvious from the fact that there exists a transformation to Weierstrass form. The singularity enhancements of Calabi-Yau manifolds with two sections were studied systematically in [10].

In this work, we aim to extend the effort of [26] and provide a new method for bringing a large class of complete intersection fibers into Weierstrass form. This class contains both models without section and with section(s). As alluded to above, we compute the Weierstrass form of the associated Jacobian in the cases which do not have a section. We develop the algorithm in Section 3 after giving a short summary of some of the mathematical background in Section 2. In Section 4 we then review complete intersections in toric varieties and, as an application of our algorithm, classify all toric Mordell-Weil groups of the 3134 nef partitions of the 4319 three-dimensional reflexive polytopes. Since the full list of results is too long to be included in the text of this paper, we have created a website at

`http://wwwth.mpp.mpg.de/members/jkeitel/Weierstrass/` (1.3)

with a database of the 3134 nef partitions of three-dimensional reflexive polyhedra, their Weierstrass forms, toric Mordell-Weil groups and generic non-Abelian singularities. Finally, in Section 5 we showcase several example manifolds that exhibit features not present for elliptic fibers that are hypersurface. Among these are a manifold with Mordell-Weil torsion $\mathbb{Z}_4$ and an F-theory model with discrete gauge group $\mathbb{Z}_4$. Furthermore we demonstrate that considering complete intersection fibers indeed evades the no-go theorem of [16] and present the first torically realized $SU(5) \times U(1)^2$ model with distinctly charged antisymmetric matter representations.

2 Koszul and Residues

The one indispensable tool for studying complete intersections is the Koszul complex and the associated hypercohomology spectral sequence. In the interest of a self-contained presentation let us quickly review these. Of course we have nothing new to say about these [27], the cognoscenti are advised to skip to Section 3.

The simplest way to think of line bundle valued cohomology groups $H^k\big(\mathbb{P}^d, \mathcal{O}(n)\big)$ is as holomorphic degree-k differential forms that transform like degree-n homogeneous polynomials

under rescalings of the homogeneous coordinates. More generally, we can consider multiple homogeneous rescalings which just amounts to a toric variety X and line bundle $\mathcal{L}$. Then $H^k(X,\mathcal{L})$ are holomorphic degree-k differential forms, transforming like homogeneous polynomials whose degree of homogeneity determined by the line bundle $\mathcal{L}$. Ultimately we are interested in a Calabi-Yau submanifold $Y \subset X$ cut out by two[2] transverse polynomials $p_1 = p_2 = 0$. There are three ways to obtain a degree-k differential form on Y:

1. Restriction of a degree-k form on X,
2. Residue integration of a degree-$(k+1)$ form around a small circle around either $p_1 = 0$ or $p_2 = 0$, and
3. Two-fold residue integration around $p_1 = p_2 = 0$ of a degree-$(k+2)$ form.

It is convenient to define the residue operators $\text{Res}_j(\omega) = \frac{1}{2\pi i}\oint \frac{(p_j\omega)}{p_j}$ and split the potential contributions $E_1^{p,q}$ to $H^{p+q}(Y,\mathcal{L}|_Y)$ into $(-p)$-fold residues of q-forms. Note the minus sign in the definition of p, as the residue operator has differential degree -1. We also have to be careful with the degree under homogeneous rescalings, as the residue operator Res_j has us multiply by the homogeneous polynomial p_j. The polynomial p_j defines a divisor $D_j = V(p_j) = \{p_j = 0\}$, and the cohomology groups of the line bundle $\mathcal{O}(D_j)$ precisely involve differential forms of the same degree of homogeneity as p_j. Hence, the residue operator actually maps

$$\text{Res}_j : \; H^{k+1}\big(X,\mathcal{L}(-D_j)\big) \longrightarrow H^k\big(Y,\mathcal{L}|_Y\big) \tag{2.1}$$

Putting everything together, the potential contributions to the cohomology for a 3-dimensional toric variety X fill out the tableau

$E_1^{p,q}(\mathcal{L}) =$

	$p=-2$	$p=-1$	$p=0$
$q=3$	$H^3\big(X,\mathcal{L}(-D_1-D_2)\big)$	$H^3\big(X,\mathcal{L}(-D_1)\big)\oplus H^3\big(X,\mathcal{L}(-D_2)\big)$	$H^3(X,\mathcal{L})$
$q=2$	$H^2\big(X,\mathcal{L}(-D_1-D_2)\big)$	$H^2\big(X,\mathcal{L}(-D_1)\big)\oplus H^2\big(X,\mathcal{L}(-D_2)\big)$	$H^2(X,\mathcal{L})$
$q=1$	$H^1\big(X,\mathcal{L}(-D_1-D_2)\big)$	$H^1\big(X,\mathcal{L}(-D_1)\big)\oplus H^1\big(X,\mathcal{L}(-D_2)\big)$	$H^1(X,\mathcal{L})$
$q=0$	$H^0\big(X,\mathcal{L}(-D_1-D_2)\big)$	$H^0\big(X,\mathcal{L}(-D_1)\big)\oplus H^0\big(X,\mathcal{L}(-D_2)\big)$	$H^0\big(X,\mathcal{L}\big)$

$$\Rightarrow H^{p+q}(Y,\mathcal{L}|_Y). \tag{2.2}$$

with the map to H^{p+q} being either $\text{Res}_1\,\text{Res}_2$, $\text{Res}_1 \oplus \text{Res}_2$, or restriction for the three respective columns. That way, the entries along the diagonal can contribute to $H^{p+q}(Y,\mathcal{L}|_Y)$, but we have no reason to believe that these are all independent.

[2]The whole discussion of this section generalizes to arbitrary codimension, but for simplicity we restrict ourselves to codimension two.

In particular, the restrictions of two different k-forms α_1, α_2 may very well be cohomologous on Y, even if they are not on X. Clearly, this is the case when $\alpha_1 - \alpha_2 = d\,\mathrm{Res}(\omega)$ for some k-form ω. Similarly, two forms on Y that came from different residues might be related by a double residue. This is implemented by a nilpotent[3] differential $d_1 : E_1^{p,q} \to E_1^{p+1,q}$. Only the cohomology with respect to d_1 has a chance of contributing to $H^{p+q}(Y, \mathcal{L}|_Y)$. We arrange the d_1-cohomology groups in the E_2-tableau

$$E_2^{p,q} = \frac{\ker\left(d_1 : E_1^{p,q} \to E_1^{p+1,q}\right)}{\mathrm{img}\left(d_1 : E_1^{p-1,q} \to E_1^{p,q}\right)}. \tag{2.3}$$

Unfortunately, this is not the end of it and even a d_1-cohomology class need not survive to a non-zero element of $H^{p+q}(Y, \mathcal{L}|_Y)$. This is the case when two different k-forms α_1, α_2 on X are related via a double residue of a $(k+1)$-form, $\alpha_1 - \alpha_2 = d\,\mathrm{Res}_1\,\mathrm{Res}_2(\omega)$. This is implemented by yet another nilpotent differential $d_2 : E_2^{p,q} \to E_2^{p+2,q-1}$. Its cohomology forms the entries of the E_3-tableau.

In general, a spectral sequence is an infinite sequence of tableaux $E_i^{p,q}$ and differentials $d_i : E_i^{p,q} \to E_i^{p+i,q+1-i}$. In the case of a two-fold complete intersection, this process stabilizes at $E_3 = E_\infty$ because all higher differentials are starting or ending outside of the 3×4 region with the non-zero entries. The diagonals of the E_∞ tableau are a filtration of the cohomology groups $H^{p+q}(Y, \mathcal{L}|_Y)$. In particular, this implies that

$$\dim H^k(Y, \mathcal{L}|_Y) = \sum_{p+q=k} \dim E_\infty^{p,q} \tag{2.4}$$

and therefore one can reconstruct the dimension of the line bundle cohomology groups on the complete intersection from the knowledge of the dimensions of the E_∞ tableau entries.

3 Weierstrass Form for Complete Intersections

In this section, we develop an algorithm to bring an elliptic curve defined by a complete intersection into Weierstrass form. The underlying idea is spelled out in Subsection 3.1. In Subsection 3.2 and Subsection 3.3 we discuss the relations between the line bundles on the complete intersection and the line bundles on the ambient space. Using an explicit example, we show in Subsection 3.4 explicitly how to apply our algorithm in practice. Finally, in Subsection 3.6 we manually compute the Weierstrass forms for the only two codimension two examples to which the algorithm cannot be applied.

3.1 Basic Algorithm

We are interested in finding the Weierstrass form of an elliptic curve over a base field that is not necessarily algebraically closed. In particular, if the base field is the function field of the base

[3] That $d_1^2 = 0$ requires a suitable sign choice; Schematically $d_1^{p=-2} = (p_1, p_2)$ and $d_1^{p=-1} = \left(\begin{smallmatrix} -p_2 \\ p_1 \end{smallmatrix}\right)$.

then this includes the case of elliptic fibrations. There are two different ways of quantifying how complicated the ambient space is: One is going from hypersurfaces to complete intersections to general subvarieties whose number of defining equations exceeds their codimension. This is convenient for constructing smooth Calabi-Yau manifolds, since we can often use genericity of the defining equations to argue that a generic subvariety is smooth. As far as an embedded elliptic curve is concerned, the choice of an ambient space leads to a particular choice of line bundle. Usually, not all line bundles on the elliptic curve are restrictions of line bundles on the ambient space; Instead, there will be some integer $d \in \mathbb{Z}_{>0}$ such that only line bundles $\mathcal{L}$ with $c_1(\mathcal{L}) \in d \cdot \mathbb{Z}$ come from the ambient space. And this integer, called the *degree*, is another measure for how complicated the ambient space is. In the remainder of this section, we will always take $\mathcal{L}$ to be a line bundle of minimal (positive) first Chern class d.

The degree is loosely related with how complicated the embedding is. In the case of a hypersurface in a two-dimensional toric variety,[4] there are 16 different ambient spaces corresponding to the 16 reflexive polygons. These realize embeddings of degree up to three, the prototypical examples are [26]:

$d = 1$: Long Weierstrass form eq. (1.2) in weighted projective space $\mathbb{P}^2[1, 2, 3]$,

$d = 2$: Hypersurface in $\mathbb{P}^2[1, 1, 2]$, and

$d = 3$: Cubic in $\mathbb{P}^2$.

If we further consider elliptic curves as complete intersections of two hypersurface equations in a three-dimensional toric variety, then there is one additional case:

$d = 4$: Complete intersection of two quadrics in $\mathbb{P}^3$.

The Weierstrass form of the equation (of the Jacobian) can in each case be derived from the relations between sections of powers of the minimal line bundle $\mathcal{L}$, see [2, 28]. We have implemented the known formulas [29] in [30].

However, this does not completely solve the problem of transforming the toric equation(s) into Weierstrass form. A general formula would just depend on the coefficients of the defining equations. For the sake of being explicit, consider a Calabi-Yau hypersurface. Clearly, we do not need a separate formula for each ambient space: More constrained hypersurface equations are the result of setting certain coefficients to zero, corresponding to the embedding of smaller dual polytopes into larger polytopes. However, already for the case of hypersurface elliptic curves of degree $d = 2$, there are two maximal dual toric polygons [26] (dually, there are two minimal polygons): $\mathbb{P}^2[1, 1, 2]$ and $\mathbb{P}^1 \times \mathbb{P}^1$. Correspondingly, there are two different formulas [26, 31] for the Weierstrass form for a toric hypersurface in the degree-2 case, without one being a special case of the other. On the plus side, though, such an equation can always be derived by looking at a particular relation between suitable sections of the "minimal" line bundle $\mathcal{L}$ and some of its powers, and this is the path we will take in this paper.

[4] Or: a toric elliptic fibration whose generic ambient space fiber is one of the 16 reflexive polygons.

3.2 Sections of Line Bundles

Before we derive equations for the relations between line bundles, we have to discuss how to work with sections in the toric setting. In the toric hypersurface case, we are familiar with the long exact sequence of sheaf cohomology when restricting to a divisor (the divisor being the hypersurface). For a complete intersection $Y \subset X$ of two equations, that is, sections of $\mathcal{O}(D_1)$ and $\mathcal{O}(D_2)$, the analogous Koszul resolution of the structure sheaf is

$$0 \longrightarrow \underbrace{\mathcal{O}_X(-D_1-D_2)}_{\mathcal{R}^{-2}} \longrightarrow \underbrace{\mathcal{O}_X(-D_1)\oplus\mathcal{O}_X(-D_2)}_{\mathcal{R}^{-1}} \longrightarrow \underbrace{\mathcal{O}_X}_{\mathcal{R}^{0}} \longrightarrow \mathcal{O}_Y \longrightarrow 0. \tag{3.1}$$

A long exact sequence is just a spectral sequence whose E_1 tableau has only two non-zero adjacent columns. Now, we have *three* columns $q = -2, -1, 0$ in the spectral sequence

$$E_1^{p,q} = H^q(X, \mathcal{L}\otimes\mathcal{R}^p) \quad \Rightarrow \quad H^{p+q}(X, \mathcal{L}\otimes\mathcal{O}_Y) = H^{p+q}(Y, \mathcal{L}|_Y). \tag{3.2}$$

The first differential d_1 is just the induced map of eq. (3.1) on the sheaf cohomology groups as familiar from the hypersurface case. However, we now have two new effects to consider:

- There are *three* sources for sections of the line bundle $\mathcal{L}_Y$ restricted to the complete intersection, namely

$$\bigoplus_p E_1^{p,-p} = H^2(X, \mathcal{L}\otimes\mathcal{R}^{-2}) \oplus H^1(X, \mathcal{L}\otimes\mathcal{R}^{-1}) \oplus H^0(X, \mathcal{L}). \tag{3.3}$$

- There is a higher differential $d_2 : H^1(X, \mathcal{L}\otimes\mathcal{R}^{-2}) \to H^0(X, \mathcal{L})$ that will identify sections of $\mathcal{L}$ beyond the obvious identifications (coming from d_1).

The first point is a general problem when studying algebraic varieties as embedded subvarieties. The sections of a line bundle $\mathcal{L}|_Y$ may or may not extend to sections of $\mathcal{L}$ over the whole ambient space $X \supset Y$. If that is not the case, then the choice of ambient space was an inconvenient one. One should either look for a different ambient space to embed into, or for a different line bundle on the ambient space whose sections behave more favorably. As we will see, in all codimension-two complete intersections there is at least one favorable line bundle, that is, of low enough degree ≤ 4 but with all required sections being induced from the ambient space, such that we can use it to construct the Weierstrass form.

3.3 The Second Differential

Consider a nef partition $-K = D_1 + D_2$ of the anticanonical divisor of the three-dimensional ambient toric variety into two numerically effective divisors D_1 and D_2. The complete intersection elliptic curve Y is defined by two polynomials p_1, p_2 as

$$Y = V(p_1) \cap V(p_2), \quad p_1 \in H^0(X, D_1), \quad p_2 \in H^0(X, D_2)\,, \tag{3.4}$$

Homogeneous coordinate	x_0	x_1	y_0	y_1	y_2
Vertex of ∇	$\begin{pmatrix}1\\0\\0\end{pmatrix}$	$\begin{pmatrix}-1\\0\\0\end{pmatrix}$	$\begin{pmatrix}0\\1\\0\end{pmatrix}$	$\begin{pmatrix}0\\0\\1\end{pmatrix}$	$\begin{pmatrix}0\\-1\\-1\end{pmatrix}$

Table 1: *The toric variety* $\mathbb{P}^1 \times \mathbb{P}^2$.

where $V(p)$ denotes the divisor defined by $p = 0$. A section s of a line bundle $\mathcal{L}$ always defines a section s_Y of $\mathcal{L}|_Y$ by restriction, but different sections on X might yield the same section on Y. Clearly, we can add any section vanishing on Y to s without changing the restriction. The obvious candidates of sections of $\mathcal{L}$ vanishing on Y are the image

$$d_1 : H^0\big(X, \mathcal{L} \otimes \mathcal{O}(-D_1)\big) + H^0\big(X, \mathcal{L} \otimes \mathcal{O}(-D_2)\big) \xrightarrow{\binom{p_1}{p_2}} H^0(X, \mathcal{L}) \tag{3.5}$$

Hence, the easy identifications just boil down to working with the quotient by the image of d_1.

What this section is concerned about is another identification that we have to perform on the sections on the ambient space, coming from the d_2 differential. To clarify this, we will look at an explicit example. In fact, the example is very simple. Consider $\mathbb{P}^1 \times \mathbb{P}^2$ with the non-product nef partition $D_1 = \mathcal{O}(1,1)$, $D_2 = \mathcal{O}(1,2)$. We let x_0, x_1 be the two homogeneous coordinates on $\mathbb{P}^1$ and y_0, y_1, y_2 be the three homogeneous coordinates on $\mathbb{P}^2$. The toric data is also summarized in Table 1. A particularly simple choice of equations that nevertheless defines a smooth complete intersection is

$$\begin{aligned} p_1 &= x_0(y_0 + y_1) + x_1 y_2 && \in H^0(\mathbb{P}^1 \times \mathbb{P}^2, D_1) \\ p_2 &= x_0 y_2^2 + x_1 y_0 y_1 && \in H^0(\mathbb{P}^1 \times \mathbb{P}^2, D_2). \end{aligned} \tag{3.6}$$

We now need to pick a line bundle $\mathcal{L}$ on the ambient $\mathbb{P}^1 \times \mathbb{P}^2$. The lowest degree choice would be $\mathcal{O}(1,0)$, which has degree 2. However, it has not enough sections on the ambient space. For example, we would need all four[5] sections of $\mathcal{O}(1,0)^2|_Y = \mathcal{O}(2,0)|_Y$ to define the z-coordinate in the Weierstrass model, but $\dim H^0(\mathbb{P}^1 \times \mathbb{P}^2, \mathcal{O}(1,0)) = 3$. Hence, we are led to look at the next-smallest degree line bundle

$$\mathcal{L} = \mathcal{O}(0,1), \quad H^0\big(\mathbb{P}^1 \times \mathbb{P}^2, \mathcal{L}\big) = \text{span}\{y_0,\ y_1,\ y_2\} \tag{3.7}$$

It is easy to see that the three sections of $\mathcal{L}$ restrict to a basis of three independent sections of $H^0(Y, \mathcal{L}|_Y)$ on the complete intersection. We also remind the reader that the Weierstrass form in the degree-3 case arises as the one relation between the ten cubic monomials $\text{Sym}^3 H^0(Y, \mathcal{L}|_Y)$

[5] A degree-d line bundle, $d > 0$, on an elliptic curve Y has of course d sections.

inside the nine-dimensional $H^0(Y, \mathcal{L}^3|_Y)$. The first tableau of the spectral sequence eq. (3.2) is

$$E_1^{p,q}(\mathcal{L}^3) = H^q(X, \mathcal{L}^3 \otimes \mathcal{R}^p) = \begin{array}{c|ccc} q{=}3 & 0 & 0 & 0 \\ q{=}2 & 0 & 0 & 0 \\ q{=}1 & \mathbb{C} & 0 & 0 \\ q{=}0 & 0 & 0 & \mathbb{C}^{10} \\ & p{=}{-}2 & p{=}{-}1 & p{=}0 \end{array} \Rightarrow H^{p+q}(Y, \mathcal{L}^3|_Y). \tag{3.8}$$

Clearly, the relation among the ten sections of $H^3(\mathbb{P}^1 \times \mathbb{P}^2, \mathcal{L}^3)$ is not coming from d_1 because the domain vanishes, see eq. (3.5). Instead, we have to quotient by the image of d_2, which is clearly equivalent to knowing the Weierstrass form of the equation. But we do not know the Weierstrass form yet! Hence we have to go back to the geometry and use a different approach to find the relations between the sections.

3.4 An Algorithm to Compute Relations

Instead, we propose to directly compute the relation between the sections on the ambient space by restricting to all affine coordinate patches. Clearly, two sections are equal if they are equal in every affine patch. In any given patch we can use a local trivialization to write the sections as polynomials, and polynomials are equal if and only if their difference is in the ideal generated by the inhomogenized defining equations. For example, consider the patch $x_1 = y_2 = 1$ in the example of Subsection 3.3. As it turns out, we only have to consider this single patch in this particular example. The inhomogenized defining equations define the ideal

$$I = \langle \hat{x}_0(\hat{y}_0 + \hat{y}_1) + 1,\ \hat{x}_0 + \hat{y}_0\hat{y}_1 \rangle = \langle \hat{x}_0\hat{y}_1^2 - \hat{x}_0^2 + \hat{y}_1,\ \hat{x}_0\hat{y}_0 + \hat{x}_0\hat{y}_1 + 1,\ \hat{y}_0\hat{y}_1 + \hat{x}_0 \rangle, \tag{3.9}$$

where the second set of generators forms a degrevlex[6] Gröbner basis and we have denoted the inhomogeneous coordinates by hats. The ten cubics generating $\operatorname{Sym}^3 H^0(Y, \mathcal{L}|_Y)$ are, in inhomogeneous coordinates,

$$\left\{ \hat{y}_0^3,\ \hat{y}_0^2\hat{y}_1,\ \hat{y}_0\hat{y}_1^2,\ \hat{y}_1^3,\ \hat{y}_0^2,\ \hat{y}_0\hat{y}_1,\ \hat{y}_1^2,\ \hat{y}_0,\ \hat{y}_1,\ 1 \right\}, \tag{3.10}$$

and their normal form modulo I is

$$\left\{ \hat{y}_0^3,\ \hat{x}_0\hat{y}_1 + 1,\ -\hat{x}_0\hat{y}_1,\ \hat{y}_1^3,\ \hat{y}_0^2,\ -\hat{x}_0,\ \hat{y}_1^2,\ \hat{y}_0,\ \hat{y}_1,\ 1 \right\}. \tag{3.11}$$

Hence, the single relation between the ten sections, after restricting them to the complete intersection and restoring the homogeneous coordinates, is

$$y_0^2 y_1 + y_0 y_1^2 - y_2^3 = 0 \tag{3.12}$$

This is now the well-known case of a cubic in three homogeneous variables. Its Weierstrass form is

$$Y^2 = X^3 + \tfrac{1}{4}, \tag{3.13}$$

which has discriminant $\Delta = \frac{27}{16}$ and j-invariant 0.

[6] That is, a degree reverse lexicographic Gröbner basis.

3.5 Kodaira Map

We still have considerable freedom in choosing the line bundle $\mathcal{L}$ which realizes the Weierstrass form as the relation between (powers of) its sections. This is nothing but the Kodaira map. For example, in the degree-3 case the three sections of $\mathcal{L}$ just realize the Kodaira embedding of the elliptic curve Y in $\mathbb{P}^2$. For the purpose of finding the Weierstrass form, we want the degree to be as small as possible, and in particular ≤ 4. However, as we essentially study the elliptic curve through its Kodaira map, we can only consider line bundles of positive degree. Otherwise the Kodaira map would shrink Y to a point, which obviously would not retain any information. Therefore, a good starting point for looking for line bundles $\mathcal{L}$ on the ambient toric variety is the cone in $H^2(X,\mathbb{Z})$ of line bundles with at least one section. This cone is generated by the first Chern classes of divisors $V(z_i)$ cut out by a single homogeneous coordinate. The degree on Y is a linear form

$$\deg(\mathcal{L}|_Y) = \int_X D_1 D_2 \; c_1(\mathcal{L}), \tag{3.14}$$

so it is just a question of enumerating weighted integer vectors to list them all up to a certain degree bound.

3.6 Two Exceptions

It turns out that there are only two nef partitions (out of 3134) for which the above algorithm fails, that is, there is no line bundle on the ambient toric variety such that

- The degree $\deg(\mathcal{L}|_Y) \leq 4$, and
- All required[7] sections for finding the Weierstrass form are restrictions of sections from the ambient space.

The two exceptions have the PALP nef ids $(4,3)$ and $(29,2)$[8]. We start with the former, which is just $\mathbb{P}^1 \times \mathbb{P}^2$ with the nef partition $D_1 = \mathcal{O}(2,1)$ and $D_2 = \mathcal{O}(0,2)$. Again using $[x_0 : x_1] \in \mathbb{P}^1$ and $[y_0 : y_1 : y_2] \in \mathbb{P}^2$ as homogeneous coordinates, the two defining polynomials are

$$\begin{aligned} p_1 &= \sum_{i=0}^{2} (a_{00i} x_0^2 + a_{01i} x_0 x_1 + a_{11i} x_1^2) y_i \,, \\ p_2 &= \sum_{i,j=0}^{2} b_{ij} y_i y_j = \begin{pmatrix} y_0 & y_1 & y_2 \end{pmatrix} \begin{pmatrix} b_{00} & b_{10} & b_{20} \\ b_{01} & b_{11} & b_{21} \\ b_{02} & b_{12} & b_{22} \end{pmatrix} \begin{pmatrix} y_0 \\ y_1 \\ y_2 \end{pmatrix} . \end{aligned} \tag{3.15}$$

Projection onto the $\mathbb{P}^1$ factor defines a map $Y = V(\langle p_1, p_2 \rangle) \to \mathbb{P}^1$. Its pre-image consists of two points: For fixed $[x_0 : x_1] \in \mathbb{P}^1$, the first equation p_1 is a line and the second equation p_2 is

[7] For degree-1, we require the sections of $\mathcal{L}$, $\mathcal{L}^2$, $\mathcal{L}^3$, and $\mathcal{L}^6$. For degree-2, we require $\mathcal{L}$, $\mathcal{L}^2$, and $\mathcal{L}^4$. For degree-3, we require $\mathcal{L}$ and $\mathcal{L}^3$. For degree-4, we require $\mathcal{L}$ and $\mathcal{L}^2$.

[8] For an explanation of the notation for the nef ids see Subsection 4.2.

a conic in $\mathbb{P}^2$, which necessarily intersect in two points. These two points can degenerate to a single point with multiplicity two, and they must do so at precisely four pre-images because a torus is the double cover of $\mathbb{P}^1$ branched at four branch points. In other words, the discriminant $\delta_{\mathbb{P}^1}$ of the double cover $Y \to \mathbb{P}^1$ is a quartic in the variables x_0, x_1 with coefficients involving a's and b's but no y's.

The form of the discriminant is constrained by symmetry; $SL(2,\mathbb{C})\times SL(3,\mathbb{C})$ acts naturally on the ambient space. The complete intersection Y is not invariant under this symmetry, but its Weierstrass form must be. More formally, we can combine the action on the homogeneous coordinates with an action on the coefficients such that the combined action does not change the equations p_1, p_2. For example, the $M_3 \in SL(3,\mathbb{C})$-part of the action is

$$\begin{pmatrix} y_0 \\ y_1 \\ y_2 \end{pmatrix} \mapsto M_3 \begin{pmatrix} y_0 \\ y_1 \\ y_2 \end{pmatrix}, \quad \begin{pmatrix} a_{ij0} \\ a_{ij1} \\ a_{ij2} \end{pmatrix} \mapsto M_3^{-1} \begin{pmatrix} a_{ij0} \\ a_{ij1} \\ a_{ij2} \end{pmatrix}, \quad (b_{ij}) \mapsto (M_3^{-1})^T (b_{ij}) M_3^{-1}. \tag{3.16}$$

A *covariant* is a polynomial that does not transform under the combined group action, obvious examples are p_1 and p_2. An *invariant* is a covariant that, furthermore, does not depend on the homogeneous coordinates, for example $\det(b_{ij})$. The discriminant δ_1 that we are looking for must be a covariant of bi-degree $(4,0)$ in $[x_0 : x_1]$ and $[y_0 : y_1 : y_2]$.

The tersest way to characterize δ_1 completely is as the Θ'-invariant [32, 33] of the system of two conics (p_1^2, p_2). That is, ignore the action on the $\mathbb{P}^1$ factor for the moment and consider p_1^2 and p_2 as two quadratics in $[y_0 : y_1 : y_2]$. The determinant Δ of the coefficient matrix of a quadratic is clearly an invariant of the action on $\mathbb{P}^2$, hence so is every ϵ-coefficient in the formal expansion[9]

$$\Delta(p_1^2 + \epsilon p_2) = \Delta(p_1^2) + \epsilon\Theta(p_1^2, p_2) + \epsilon^2\Theta'(p_1^2, p_2) + \epsilon^3\Delta(p_2) \tag{3.17}$$

We note that $\delta_1(x_0, x_1) = \Theta'(p_1^2, p_2)$ is quartic in x_0 and x_1, quadratic in the coefficients a_{ijk} and quadratic in the coefficients b_{ij}. Finally, the equation of a double cover branched at the zeroes of δ_1 is

$$Y^2 = \delta_1(x_0, x_1), \tag{3.18}$$

for which we already know how to write the Weierstrass form [29, 30].

It remains to consider the second exceptional case, that is, the one with PALP nef id $(29, 2)$. Geometrically, it is the product $\mathbb{P}^1 \times dP_1$, that is, a simple blowup[10] of the first case along a curve $\mathbb{P}^1 \times \{\text{pt.}\}$. Moreover, the two divisors defining the nef partition are just the pull-backs of the two divisors of the first case. In terms of toric geometry, this means that the dual polytope ∇ contains the dual polytope of $\mathbb{P}^1 \times \mathbb{P}^2$. Dually, the polytope Δ is contained in the polytope of $\mathbb{P}^1 \times \mathbb{P}^2$. Hence the formula for bringing the complete intersection into Weierstrass form is simply a specialization of the formula from the first case where some coefficients are set to zero.

[9] The invariants $\Delta(p_1^2)$ and $\Theta(p_1^2, p_2)$ vanish because p_1^2 is a degenerate conic.

[10] We use the notation where $\mathbb{P}^2 = dP_0$.

4 Classifying Toric Mordell-Weil Groups

We begin this section by reviewing how to construct Calabi-Yau manifolds as complete intersections in toric varieties. Having laid the general groundwork, we then calculate all nef partitions of three-dimensional reflexive polytopes and give a short summary of our results. Next, we recall the concept of *toric* Mordell-Weil groups as introduced in [16] and explain how to compute them for a given ambient fiber space. Finally, we determine the toric Mordell-Weil group for every elliptic fiber embedded in a three-dimensional toric variety corresponding to a reflexive polytope and comment on our results.

4.1 Complete Intersections in Toric Varieties

As discovered by Batyrev [34, 35], toric geometry provides a convenient way of constructing Calabi-Yau manifolds embedded in ambient toric varieties either as hypersurfaces or as complete intersections. Conveniently, Batyrev's construction is combinatorial: Given a lattice polytope Δ in a lattice $N \simeq \mathbb{Z}^{n+1}$, its dual (or polar) polytope is given by

$$\Delta^\circ := \{y \in M | \langle x, y\rangle \geq -1 \ \forall x \in \Delta\}\,. \tag{4.1}$$

Here M is the dual lattice of N. If Δ° is again a lattice polytope, then Δ is called *reflexive*. Furthermore, since $(\Delta^\circ)^\circ = \Delta$, Δ° is reflexive if and only if Δ is reflexive. Next, we take all lattice points of Δ° that are not interior points of a facet[11] to construct a fan from a fine star triangulation of these points with respect to the origin and call the corresponding toric variety X_{n+1}. Denote the homogeneous coordinates of X_{n+1} by z_i and the respective points of Δ° by x_i. Consider then the hypersurface Y_n inside X_{n+1} given by the equation

$$p = \sum_{y_j \in \Delta} a_j \prod_i z_i^{\langle y_j, x_i\rangle + 1}\,. \tag{4.2}$$

It defines a Calabi-Yau n-fold inside X_{n+1} and there exist simple combinatorial formulas in terms of the data of Δ and Δ° to compute its cohomology dimensions. Furthermore, it is worth to note that by exchanging Δ and Δ° one obtains the mirror manifold of Y_n.

To generalize this approach to complete intersections, one must specify additional information. In the hypersurface case, the homology class of the divisor defined by the vanishing of (4.2) must be Poincaré-dual to the cohomology class of the first Chern class of the ambient space in order for the hypersurface to be Calabi-Yau. If instead the Calabi-Yau manifold is to be the intersection of several divisors, then their sum must still be dual to the first Chern class of the ambient space. However, the classes of the individual divisors are not fixed anymore.

One such way of additionally specifying the classes of the divisors defining the complete intersection proceeds by giving a *nef partition* of the reflexive polytope Δ°. A nef partition of

[11] That is, a face of codimension one.

Δ° into r parts is a set of lattices polytopes Δ_i and ∇_i with $i = 1, \ldots, r$ satisfying

$$\begin{aligned} \Delta &= \Delta_1 + \cdots + \Delta_r & \Delta^\circ &= \langle \nabla_1, \ldots, \nabla_r \rangle_{\text{conv}} \\ \nabla^\circ &= \langle \Delta_1, \ldots, \Delta_r \rangle_{\text{conv}} & \nabla &= \nabla_1 + \cdots + \nabla_r \end{aligned} \tag{4.3}$$

with $\langle \cdot, \ldots, \cdot \rangle_{\text{conv}}$ the convex hull, $+$ Minkowski addition, and

$$(\nabla_n, \Delta_m) \geq -\delta_{nm} \,, \tag{4.4}$$

where here we mean this to hold for every pair of points from ∇_n and Δ_m. Effectively, we have split the vertices of Δ° into r disjoint subsets spanning the polytopes ∇_i and made sure that they fulfill certain additional constraints. Given such a nef partition, we again define X_{n+r} to be the ambient variety obtained from Δ° as above. Furthermore, the nef partition specifies the following r equations defining the Calabi-Yau manifold Y_n:

$$p_m = \sum_{y_j \in \Delta_m} a_{m,j} \prod_{n=1}^{r} \prod_{x_i \in \nabla_n} z_i^{\langle y_j, x_i \rangle + \delta_{nm}} \,, \qquad m = 1, \ldots, r \,. \tag{4.5}$$

Note that one can also interpret a nef partition of Δ° as a nef partition of ∇°. In doing so, one exchanges Y_n by its mirror. Let us point out that the ambient space of a mirror manifold can differ for different nef partitions of the same polytope.

Finally, we remark that there are two special cases of nef partitions. The simplest one corresponds to *direct products*. Given nef partitions of two reflexive polytopes ${\Delta^{(1)}}^\circ$ and ${\Delta^{(2)}}^\circ$, these define a nef partition of the polytope $\Delta^{(1)} \times \Delta^{(2)}$. The corresponding complete intersection manifold is then a direct product of complete intersections inside the direct product of the varieties corresponding to ${\Delta^{(1)}}^\circ$ and ${\Delta^{(2)}}^\circ$. The other special case corresponds to *projections*. If a nef partition has one component ∇_i that is spanned only by a single vertex v, then the complete intersection can be reduced to a complete intersection in a toric variety of one dimension less whose reflexive polytope is obtained by projecting Δ° along v.

4.2 Nef Partitions of 3d Lattice Polytopes

As a test sample for applying our Weierstrass algorithm we use elliptic curves that are embedded in three-dimensional toric varieties and we therefore spend a moment to construct the corresponding nef partitions. It is well-known that the number of reflexive polytopes of a given dimension is finite, but increases very quickly with the dimension: In two dimensions, there are precisely 16 reflexive polygons, in three dimensions there exist 4319 reflexive polytopes [36], and the $473,800,776$ reflexive polytopes in four dimensions were determined in [37]. The exact number in five dimensions is unknown, but expected to be large enough to currently make its computation unfeasible. In the case of the 4319 three-dimensional polytopes, the nef partitions can be computed using PALP [38] via Sage [30] within a matter of minutes. One finds that there exist 3134 nef partitions. 16 of these correspond to direct products embedded in $F_i \times \mathbb{P}^1$ for the 16 two-dimensional varieties, and 807 correspond to projections.

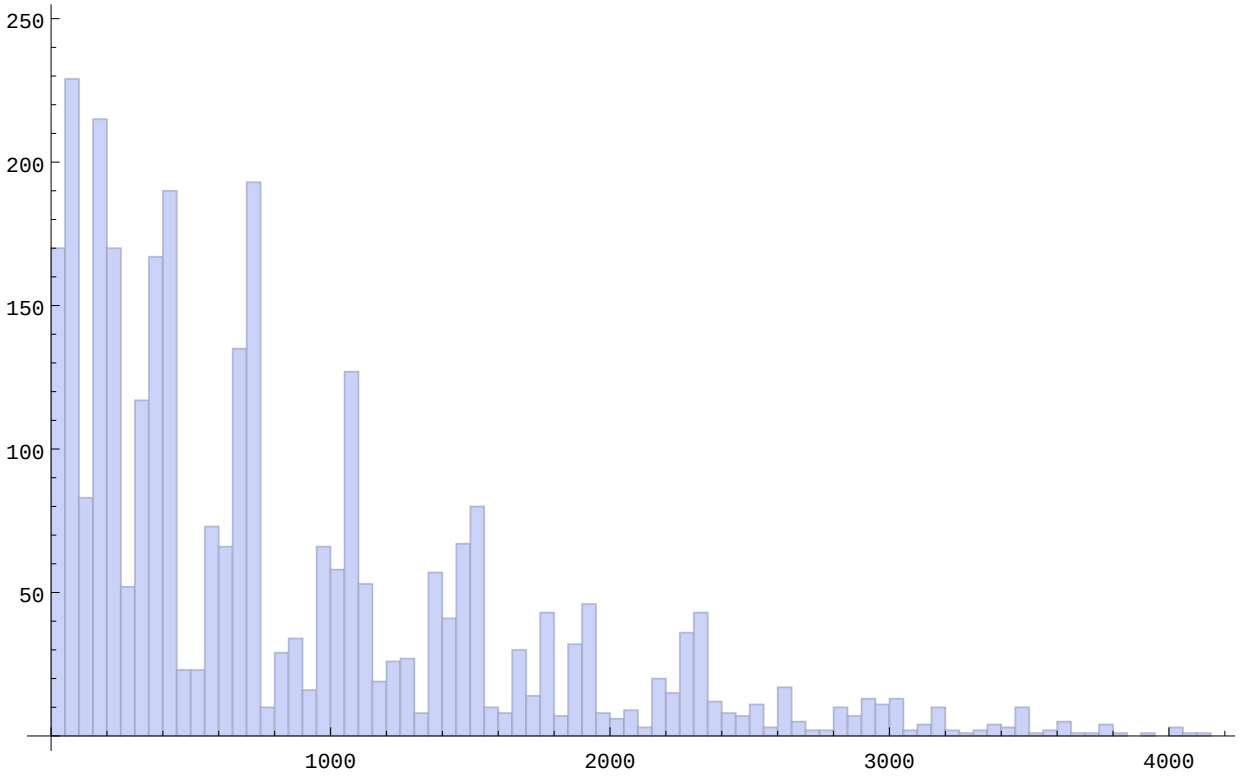

Figure 1: *Histogram of the number of nef partitions of the* 4319 *reflexive polytopes in three dimensions.*

Last but not least, let us introduce a nomenclature for denoting the nef partitions dealt with in the following subsections. Three-dimensional reflexive polytopes already have a unique id as assigned by the PALP database. This id obeys

$$\#_{\text{points}}(P) < \#_{\text{points}}(P') \quad \Rightarrow \quad id(P) < id(P') \tag{4.6}$$

and

$$\#_{\text{points}}(P) = \#_{\text{points}}(P') \ \wedge \ \#_{\text{vertices}}(P) < \#_{\text{vertices}}(P') \quad \Rightarrow \quad id(P) < id(P')\,, \tag{4.7}$$

that is, the polytopes are ordered by the number of integral points and the number of vertices. Sage can be used to compute the PALP index of a given reflexive polytope. To furthermore identify the nef partitions uniquely, we run `nef.x` via the

```
ReflexivePolytope.nef_partitions()
```
(4.8)

method of Sage on a given reflexive polytope in PALP normal form. This output is uniquely ordered and allows us to assign ids to the different nef partitions. By a nef partition with id (i, j) we therefore mean the $(j + 1)$th nef partition of the three-dimensional reflexive polytope with PALP id i as determined by the `nef_partitions()` method of Sage.

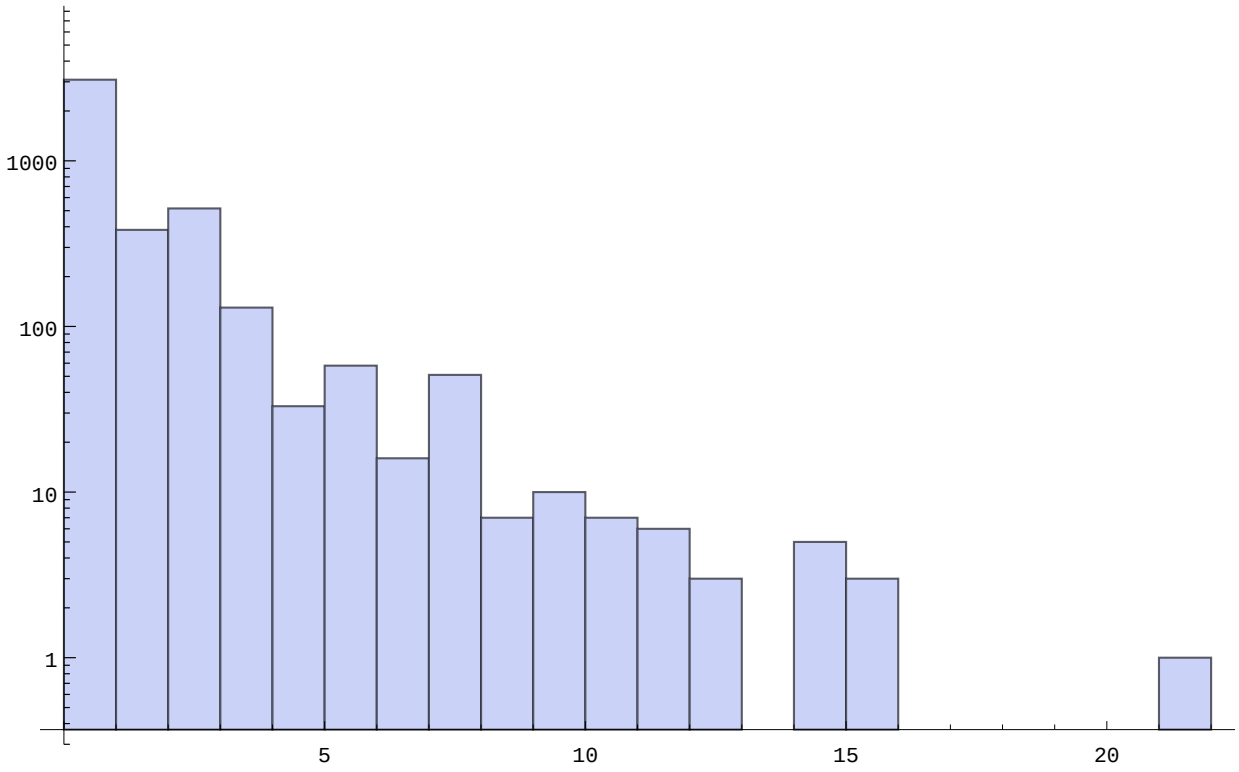

Figure 2: *Histogram of the number of polytopes that have a given number of nef partitions. There are* 3090 *reflexive three-dimensional polytopes that do not admit a nef partition. The reflexive polytope with PALP id* 214 *has the most nef partitions, namely* 21*.*

4.3 Toric Mordell-Weil Groups

Next, we introduce the concept of *toric* Mordell-Weil groups of an elliptic fiber. First however, let us quickly recall a few facts about elliptic curves. An elliptic curve is a genus-one curve, i.e. a T^2, together with one special marked point that defines the zero point of the curve. Given such an elliptic curve $E(K)$ over some field K, it is well-known that the set of points on this elliptic curve with coefficients in K forms a group, called the Mordell-Weil group $\mathrm{MW}(E)$ of the curve. The group action can easily be understood visually: In order to add two points P and Q, intersect the elliptic curve E with the line passing through both P and Q. It is guaranteed to have a third intersection with E, which we denote by R. Construct another line passing through R and the zero point of the elliptic curve. The third intersection point of this line will be $P+Q$. While it is straightforward to show that this does indeed define a valid Abelian group action[12], it is a highly non-trivial fact that the Mordell-Weil group is finitely generated.

Now we would like to consider fibrations Y_n of elliptic curves over base manifolds B_{n-1}. Non-trivial fibrations of this kind imply that the complex structure of the elliptic curve varies from point to point in the base and, equivalently, one can view such a fibration as an elliptic

[12]For special cases, a proof and expressions in coordinate form see for example [28, 39].

curve over the field of rational functions on the base manifold. With respect to this function field the rational points of the elliptic curve correspond to the global sections

$$f_i : B_{n-1} \to Y_n \tag{4.9}$$

of the fibration. In particular, for a non-singular elliptic fibration one has the relation

$$h^{1,1}(Y_n) = h^{1,1}(B_{n-1}) + \mathrm{rk}\,\mathrm{MW}(Y_n) + 1\,. \tag{4.10}$$

Here the $+1$ is owed to the fact that it takes $n+1$ independent global sections $f_1, \ldots, f_{n+1}$ in order to generate a Mordell-Weil group of rank n, since one section must serve as the zero point, or neutral element, of the elliptic fiber. If one takes f_0 as zero section, then

$$\sigma_i := f_i - f_0 \tag{4.11}$$

can be used as generators of the Mordell-Weil group.

Given a general elliptic fibration, it is a difficult problem to determine all global sections, even though their total number can be computed using (4.10) and generalizations thereof. In particular, there exist examples for which the homology classes of the sections can be determined, but their precise coordinate expressions cannot [8]. More importantly, the total Mordell-Weil group generally depends on the entire fibration and can therefore not be computed independently of the base. Nevertheless, there exists a subgroup of the Mordell-Weil group, the *toric* Mordell-Weil group, that indeed depends only on the toric variety the elliptic fiber is embedded in and can therefore be computed without reference to a specific base manifold or fibration. Let us therefore explain how the toric Mordell-Weil group is defined by reviewing the material of [16].

Denote the toric ambient fiber space by W_{1+c}, where c is the codimension of the elliptic fiber E. Then the homogeneous coordinates z_i of W_{1+c} define toric divisors $V(z_i)$ given by the vanishing of a single homogeneous coordinate. If such a divisor intersects the elliptic curve once, i.e. is satisfies

$$\int_E V(z_i) = 1\,, \tag{4.12}$$

then this divisor will become a global section of the fibration after fibering W_{1+c} over the base manifold. We call these divisors the *toric* global sections and call the subgroup

$$\mathrm{MW}_T(E) \subseteq \mathrm{MW}(E) \tag{4.13}$$

the toric Mordell-Weil group. In [16] the toric Mordell-Weil groups of elliptic curves embedded as hypersurfaces inside two-dimensional toric varieties were analyzed. In the next subsection, we will apply the same analysis using the new algorithm for Weierstrass forms developed in Section 3.

4.4 Results for Elliptic Curves of Codimension Two

In the final subsection of this chapter, we present the main results of our computations. Before proceeding to the results, let us remark on how to compute the Mordell-Weil group laws for a given fibration in practice. While we computed the Weierstrass forms of the elliptic curves by keeping the coefficients in the complete intersection equations general, this approach makes little sense for determining the Mordell-Weil group laws. Instead, we generated a considerable number[13] of curves with random complex structure coefficients in $\mathbb{Z}$. We then computed the explicit coefficients of the points cut out by toric sections, mapped these to the elliptic curve in Weierstrass form and determined the relations between them. Special care has to be taken when mapping the points from the original elliptic curve to the curve in Weierstrass form. As discussed in Section 3 our map works through an intermediate embedding inside $\mathbb{P}_{231}$, $\mathbb{P}_{112}$, $\mathbb{P}^2$, or $\mathbb{P}^3$. However, the maps from the last three spaces to Weierstrass form are not injective: They in fact map the elliptic curves $4:1$, $9:1$ and $16:1$, respectively. As a consequence, distinct points on the original curve may be mapped to the same point of the curve in Weierstrass form and therefore torsion factors of the Mordell-Weil group may get lost. To make sure that we find the correct torsion groups, it is therefore crucial to use different embeddings of the same curve in case that the points on the curve in Weierstrass satisfy non-trivial relations with respect to the Mordell-Weil group law. While the map from $\mathbb{P}^2$ to Weierstrass form may eliminate a $\mathbb{Z}_3$ torsion factor, the map from $\mathbb{P}_{112}$ will not, and one can therefore determine the correct toric Mordell-Weil groups even in the presence of torsion.

The computations were performed using PALP [38], Sage [30] and in particular the Sage modules for polytopes [40] and toric geometry [41]. Furthermore, we made heavy use of the Sage interface to Singular [42]. For every nef partition of a reflexive three-dimensional polytope Δ°, we computed the following data:

- The two defining equations of the complete intersection with general coefficients a_i.
- The Weierstrass coefficients f and g of equation (1.1) in terms of a_i.
- The integral points v_i of Δ° that are promoted to toric sections $V(z_i)$ after fibering the elliptic curve over a base manifold.
- The relations between the Mordell-Weil generators σ_i after choosing a zero point on the elliptic curve.
- The resulting toric Mordell-Weil group, including its torsion part.
- The Kodaira types of the non-toric singularities that occur if all a_i are generic.

Since the full list of results is too long to be included in the text of this paper, we have created a website at

`http://wwwth.mpp.mpg.de/members/jkeitel/Weierstrass/` (4.14)

[13] By considerable, we mean $\mathcal{O}(100)$ in order to make sure that we indeed obtain a generic example.

with a database of the 3134 nef partitions of three-dimensional reflexive polyhedra. For each such nef partition, there exists a file of the form `RP_NEF.txt`. Let us illustrate the file format using the nef partition $(2355, 0)$:

```
Summary for nef partition with id (2355, 0).

Defining data of the nef partition:
rays = [z0: (1, 0, 0), z1: (0, 1, 0), z2: (0, 0, 1), z3: (-1, 1, 1),
z4: (2, -1, -1), z5: (1, 0, -1), z6: (1, -1, 0), z7: (-1, 1, 0),
z8: (-1, 0, 1), z9: (-2, 1, 1), z10: (1, -1, -1), z11: (0, 0, -1),
z12: (0, -1, 0), z13: (-1, 0, 0)]
nabla_1 = (0, 1, 2, 3, 4, 5, 6)
nabla_2 = (7, 8, 9, 10, 11, 12, 13)

Toric Mordell-Weil group:
zero = (0, 1, 0)
generators = [s0: (0, 0, 1), s1: (2, -1, -1), s2: (-2, 1, 1),
s3: (0, 0, -1), s4: (0, -1, 0)]
relations = [s0-s3 = (1), s1-s2 = (1), s4 = (1)]
group = Z^2 x Z_2

Complete intersection equations:
p1 = a3*z0*z1*z2*z3*z4*z5*z6 + a2*z1*z3*z5*z7*z9*z11*z13
+ a1*z2*z3*z6*z8*z9*z12*z13 + a0*z4*z5*z6*z10*z11*z12*z13
p2 = a7*z0*z1*z2*z3*z7*z8*z9 + a6*z0*z1*z4*z5*z7*z10*z11
+ a5*z0*z2*z4*z6*z8*z10*z12 + a4*z7*z8*z9*z10*z11*z12*z13

Weierstrass coefficients:
f = [...]
g = [...]

Generic non-Abelian singularities:
a7: (0, 0, 2), I_2
a6: (0, 0, 2), I_2
a5: (0, 0, 2), I_2
a4: (0, 0, 2), I_2
a3: (0, 0, 2), I_2
a2: (0, 0, 2), I_2
a1: (0, 0, 2), I_2
a0: (0, 0, 2), I_2
```

The first block summarizes the toric data defining the nef partition. The first line defines

the variable names z_i assigned to the homogeneous variables associated with each ray of the ambient fan and the second line specifies the nef partition by listing the indices of the rays spanning ∇_1 and ∇_2. In this example

$$\nabla_1 = \langle v_0 v_1 v_2 v_3 v_4 v_5 v_6 \rangle_{\text{conv}} , \qquad \nabla_2 = \langle v_7 v_8 v_9 v_{10} v_{11} v_{12} v_{13} \rangle_{\text{conv}} . \tag{4.15}$$

The second paragraph contains information about the toric Mordell-Weil group. This particular example has six divisors that become (not necessarily independent) sections after fibering the elliptic curve over a base manifold and the toric Mordell-Weil group generated by these divisors is $\mathbb{Z}^2 \oplus \mathbb{Z}_2$. Choosing the divisor corresponding to the ray $\begin{pmatrix} 0 & 1 & 0 \end{pmatrix}^T$ as the divisor that cuts out the neutral element on the curve, the remaining five divisors σ_i, $i = 0, \ldots, 4$ satisfy three relations. To specify these relations we denote by (i) the generator of the torsion part times i. Here, this means that the section σ_4 generates the $\mathbb{Z}_2$ factor and, up to this torsion part, the pairs of sections σ_0 and σ_3, and σ_1 and σ_2, are identified under the Mordell-Weil group law. Next, the record contains the two complete intersection equations in order to define the coefficients a_i determining the complex structure of the elliptic curve. The Weierstrass coefficients (omitted here due to their length) are then given in terms of the a_i. Finally, we list the non-Abelian singularities that a such an elliptic curve with generically chosen a_i will have. In this case, there is an additional $SU(2)^8$ gauge group with branes located along the eight base loci $a_i = 0$ for $i = 0, \ldots 7$.

Statistics of the 3134 elliptic curves of codimension two

Let us give a quick summary of the results we found. We begin by noting that 16 of the 3134 nef partitions are direct products. Up to lattice isomorphisms, they are obtained as

$$\nabla_1 = \langle \begin{pmatrix} 1 \\ 0 \\ 0 \end{pmatrix} , \begin{pmatrix} -1 \\ 0 \\ 0 \end{pmatrix} \rangle_{\text{conv}} , \qquad \nabla_2 = \langle \begin{pmatrix} 0 \\ v_i \end{pmatrix} \text{ where } v_i \in F_j \rangle_{\text{conv}} , \tag{4.16}$$

where F_j is one of the 16 reflexive polygons. Their PALP ids are contained in Table 2. The total ambient space corresponding to the face fan of Δ° is $\mathbb{P}^1 \times F_j$ and the complete intersection factors into a quadratic equation inside $\mathbb{P}^1$ and the anticanonical hypersurface in F_j. Therefore these nef partitions consist of two disjoint elliptic curves, each of which is described by a hypersurface inside a two-dimensional toric variety. Both of them have the same complex structure. Clearly, set-ups of this kind do not occur in F-theory compactifications with fibers defined as hypersurfaces. It would be interesting to study the resulting low-energy effective theories of such compactifications further, but we reserve this for future work. As these spaces appear to make up a class of their own, we will not include them in our analyses below and instead restrict to the remaining 3118 nef partitions.

We list in Figure 3 the distribution of the number of toric divisors corresponding to sections among the complete intersection curves. Note that not all of these divisors will be independent in homology. In Figure 4 we give the distribution of the toric Mordell-Weil ranks. The highest

$\mathbb{P}^1\times$	F_1	F_2	F_3	F_4	F_5	F_6	F_7	F_8
PALP id	$(4,2)$	$(30,1)$	$(29,3)$	$(17,1)$	$(84,8)$	$(61,2)$	$(218,0)$	$(149,3)$

$\mathbb{P}^1\times$	F_9	F_{10}	F_{11}	F_{12}	F_{13}	F_{14}	F_{15}	F_{16}
PALP id	$(194,5)$	$(113,0)$	$(283,0)$	$(356,3)$	$(453,0)$	$(505,0)$	$(509,0)$	$(768,1)$

Table 2: *The PALP ids for the* 16 *nef partitions that are direct products inside the spaces* $\mathbb{P}^1 \times F_i$*, where* F_i *is a reflexive polygon.*

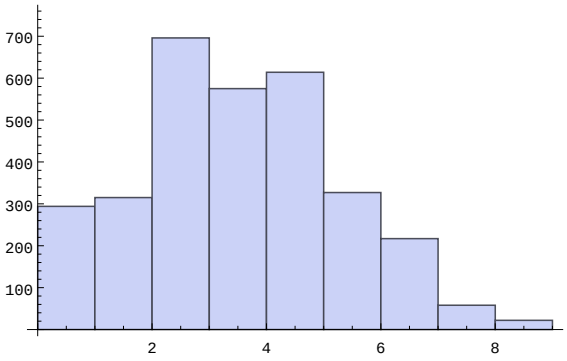

Manifolds	Toric sections
294	0
315	1
696	2
575	3
614	4
327	5
217	6
58	7
22	8

Figure 3: *Histogram of the number of toric sections for the* 3118 *nef partitions of three-dimensional reflexive polytopes that are not direct products.*

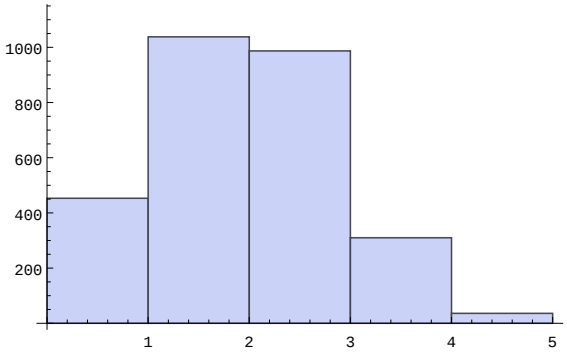

Manifolds	Mordell-Weil rank
453	0
1038	1
987	2
310	3
36	4

Figure 4: *Histogram of the toric Mordell-Weil rank for the nef partitions of three-dimensional reflexive polytopes. The* 326 *complete intersections that are either a direct product or do not have a toric section are excluded.*

Trivial group	$\mathbb{Z}_2$	$\mathbb{Z}_3$	$\mathbb{Z}_4$	$\mathbb{Z}$	$\mathbb{Z}\oplus\mathbb{Z}_2$	$\mathbb{Z}^{\oplus 2}$	$\mathbb{Z}^{\oplus 2}\oplus\mathbb{Z}_2$	$\mathbb{Z}^{\oplus 3}$	$\mathbb{Z}^{\oplus 3}\oplus\mathbb{Z}_2$	$\mathbb{Z}^{\oplus 4}$
315	113	24	1	931	107	985	2	309	1	36

Table 3: *The full toric Mordell-Weil groups for the elliptic fibers of codimension two. Note that we have omitted direct products and the genus-one curves that do not have a single toric point.*

toric rank that we find is four. Naturally, not all groups of the same rank are equal, as some have additional torsion factors. In Table 3 we give a complete survey of the toric Mordell-Weil groups for the models that possess at least one toric section. As one might expect, there are additional toric Mordell-Weil groups when compared with the elliptic curves that are embedded in toric surfaces. The groups that do not occur for elliptic curves that are hypersurfaces are

$$\mathbb{Z}_4, \quad \mathbb{Z}^{\oplus 2} \oplus \mathbb{Z}_2, \quad \mathbb{Z}^{\oplus 3} \oplus \mathbb{Z}_2, \quad \mathbb{Z}^{\oplus 4}\,. \tag{4.17}$$

Last, but not least, let us comment on the appearance of generic non-Abelian gauge groups. As noted in [16] and recently examined in detail in [17], certain fibers can generically induce non-Abelian singularities. These generic non-Abelian singularities differ from the ones induced by tops [3, 43]. When a non-Abelian singularity is enforced by a top, the ambient space of the elliptic fiber becomes reducible over a divisor in the base and as a consequence, the elliptic fiber does, too. In the case of these generic non-Abelian singularities the ambient space remains irreducible, but the fiber splits into various irreducible pieces. Such non-Abelian singularities cannot be read off directly from the toric data of the ambient space and therefore we called them *non-toric* non-Abelian singularities in [16]. Note also that the base locus over which such singularities occur is *not* defined by the vanishing of a single homogeneous coordinate, but rather a polynomial in the base coordinates.

Since these non-toric singularities are not directly visible in the defining data of the ambient space, the exceptional divisors do not belong to rays of a top, but instead to rays that are part of the fan defining the ambient space of the generic fiber. Since the maximum number of integral points of a reflexive polytope of given dimension is bounded from above, the maximum number of non-toric exceptional divisors and therefore the total rank of the non-toric gauge group is, too. To illustrate this, consider the 16 reflexive polygons. F_{16}[14] is the one with most integral points, namely ten. The nine non-zero points give rise to seven independent homology classes. One of them corresponds to the neutral element of the elliptic curve, so the maximum allowed gauge rank is six. In fact, one can show that the maximal non-toric gauge group is $SU(3)^3/\mathbb{Z}_3$ [17].

Since three-dimensional reflexive polytopes can contain more integral points than their two-dimensional analogues (the largest one has 39 integral points), the non-toric gauge group content is considerably more diverse. Not only can one find non-toric GUT candidates, but there are also fibers that generically exhibit E_6, E_7, and E_8 singularities. In Appendix A we list the non-toric singularities for the 3118 non-product nef partitions.

5 Examples

Having studied the toric Mordell-Weil groups of the elliptic curves of codimension two, the next natural step would be to classify their *tops*, i.e. all ways of generating non-Abelian singularities

[14] Here we are using the notation of [16], in which $F_{16} \cong \mathbb{P}^2/\mathbb{Z}_3$

torically. While the classification of two-dimensional tops was achieved in [44], three-dimensional tops have so far not been studied. However, as these tops appear to have a fairly involved structure, we reserve this task for future work. Instead, we present several interesting examples illustrating features that do not occur for fibers in toric surfaces.

5.1 $SU(5) \times U(1)^2$ with Different Antisymmetric Representations

Let us begin with the example that motivated this work in the first place: An $SU(5)$ GUT model with $U(1)$ factors. As mentioned in the introduction, *fully resolved* $SU(5)$ F-theory models with fibers embedded as hypersurfaces suffer from the constraint that their antisymmetric representations always have the same charge under additional $U(1)$ gauge factors. For complete intersection fibers, we do not expect this to happen anymore.

v_0	v_1	v_2	v_3	v_4	v_5
$\begin{pmatrix}1\\0\\0\end{pmatrix}$	$\begin{pmatrix}0\\1\\0\end{pmatrix}$	$\begin{pmatrix}0\\0\\1\end{pmatrix}$	$\begin{pmatrix}-1\\0\\-1\end{pmatrix}$	$\begin{pmatrix}-1\\-1\\0\end{pmatrix}$	$\begin{pmatrix}1\\1\\1\end{pmatrix}$

Table 4: *Vertices of the three-dimensional reflexive polytope with PALP id* 22.

In order to confirm the existence of multiple **10** representations, we are therefore led to consider a nef partition with non-trivial toric Mordell-Weil group. To be concrete, let us pick the following nef partition of the polytope given in Table 4:

$$\nabla_1 = \langle v_1 v_2 v_3 v_4 v_5 \rangle_{\text{conv}} \,, \qquad \nabla_2 = \langle v_0 \rangle_{\text{conv}} \,. \tag{5.1}$$

Since ∇_2 is one-dimensional, this nef partition is a *projection*. In particular, this means that we can directly solve the second equation, plug the result into the first equation and obtain the Weierstrass form of a hypersurface equation. According to the conventions of Subsection 4.2, this nef partition has the unique id $(22, 0)$. Looking it up in our classification results, we find that it has three sections, namely the divisors corresponding to the rays v_1, v_2, and v_5. Let us divisor $V(z_5)$ as the neutral element of our elliptic curve. Then $\sigma_1 = V(z_0) - V(z_5)$ and $\sigma_2 = V(z_2) - V(z_5)$ generate a $\mathbb{Z} \oplus \mathbb{Z}$ group.

Let us now write down the equations that define the complete intersection inside the three-dimensional toric variety corresponding to the reflexive polytope of Table 4. Keeping the coefficients general, the equations of the complete intersection defined by the nef partition (5.1) are

$$\begin{aligned} p_1 = {} & \tilde{a}_0 z_1^2 z_2^2 z_5^3 + \tilde{a}_1 z_1^2 z_2 z_3 z_5^2 + \tilde{a}_2 z_1 z_2^2 z_4 z_5^2 + \tilde{a}_3 z_1^2 z_3^2 z_5 + \tilde{a}_4 z_1 z_2 z_3 z_4 z_5 + \tilde{a}_5 z_2^2 z_4^2 z_5 \\ & + \tilde{a}_6 z_0 z_1 z_2 z_5^2 + \tilde{a}_7 z_1 z_3^2 z_4 + \tilde{a}_8 z_2 z_3 z_4^2 + \tilde{a}_9 z_0 z_1 z_3 z_5 + \tilde{a}_{10} z_0 z_2 z_4 z_5 + \tilde{a}_{11} z_0 z_3 z_4 + \tilde{a}_{12} z_0^2 z_5 \end{aligned} \tag{5.2}$$

$$p_2 = \tilde{b}_0 z_1 z_2 z_5 + \tilde{b}_1 z_1 z_3 + \tilde{b}_2 z_2 z_4 + \tilde{b}_3 z_0 \,. \tag{5.3}$$

Here one can see that this nef partition is indeed a projection: By solving $p_2 = 0$ for z_0 and inserting the solution in p_1 the complete intersection is reduced to a hypersurface inside the

toric variety corresponding to the polytope obtained by projecting along v_0. However, this still suffices for our purposes. Since it is the limited number of triangulations of the $SU(5)$ tops for a codimension one hypersurface that constrains the **10** charges, we are still circumventing this constraint here by considering triangulations of the higher-dimensional variety in which the elliptic curve has codimension two.

Next, we tune the $\tilde{a}_i$ and $\tilde{b}_i$ such as to enforce an $SU(5)$ singularity along the divisor $e_0 = 0$ in the base manifold. Then we resolve that singularity introducing exceptional divisors e_i, $i = 1, \ldots, 4$ and find that the coefficients $\tilde{a}_i$ and $\tilde{b}_i$ take the form

$$\begin{aligned}
&\tilde{a}_0 = a_0 \cdot e_0^3 e_1 e_2^2 e_4^2 && \tilde{a}_1 = a_1 \cdot e_0^2 e_1 e_2 e_4 && \tilde{a}_2 = a_2 \cdot e_0^2 e_1 e_2^2 e_4 \\
&\tilde{a}_3 = a_3 \cdot e_0 e_1 && \tilde{a}_4 = a_4 \cdot e_0 e_1 e_2 && \tilde{a}_5 = a_5 \cdot e_0 e_1 e_2^2 \\
&\tilde{a}_6 = a_6 \cdot e_0 e_4 && \tilde{a}_7 = a_7 \cdot e_0 e_1^2 e_2 e_3 && \tilde{a}_8 = a_8 \cdot e_0 e_1^2 e_2^2 e_3 \\
&\tilde{a}_9 = a_9 \cdot e_0 e_1 e_3 e_4 && \tilde{a}_{10} = a_{10} && \tilde{a}_{11} = a_{11} \cdot e_1 e_3 \\
& && \tilde{a}_{12} = a_{12} \cdot e_0 e_1 e_3^2 e_4^2 &&
\end{aligned} \tag{5.4}$$

and

$$\tilde{b}_0 = b_0 \cdot e_0 e_2 e_4 \qquad \tilde{b}_1 = b_1 \qquad \tilde{b}_2 = b_2 \cdot e_2 \qquad \tilde{b}_3 = b_3 \cdot e_3 e_4 \,. \tag{5.5}$$

Here a_i and b_i are polynomials in the base variables that depend on e_i only through the combination $w_0 \equiv e_0 e_1 e_2 e_3 e_4$. The toric data corresponding to this blowup are given in Table 5.

e_0	e_1	e_2	e_3	e_4
$\begin{pmatrix} 0 \\ 0 \\ 0 \\ w_0 \end{pmatrix}$	$\begin{pmatrix} -1 \\ -1 \\ -1 \\ w_0 \end{pmatrix}$	$\begin{pmatrix} -1 \\ -1 \\ 0 \\ w_0 \end{pmatrix}$	$\begin{pmatrix} 0 \\ -1 \\ -1 \\ w_0 \end{pmatrix}$	$\begin{pmatrix} 1 \\ 0 \\ 0 \\ w_0 \end{pmatrix}$

Table 5: *Torically, the blowup of (5.4) corresponds to introducing the top defined here, where w_0 is a ray of the fan of the base. The GUT brane will then be located on the divisor corresponding to w_0. Note that here we and in (5.4) we are denoting the rays and the corresponding homogeneous variables by the same letters e_i.*

As a power series in w_0, the Weierstrass coefficients read

$$f = -\frac{1}{48}\left(a_{10}^4 \cdot b_1^4 + 4 \cdot a_{10}^2 \cdot b_1^2 \cdot c_1 \cdot w_0 + c_2 \cdot w_0^2\right) + \mathcal{O}(w_0^3) \tag{5.6}$$

$$g = \frac{1}{864}\left(a_{10}^6 \cdot b_1^6 + 6 \cdot a_{10}^4 \cdot b_1^4 \cdot c_1 \cdot w_0 + 3 b_1^2 \cdot a_{10}^2 \cdot c_3 \cdot w_0^2 + c_4 \cdot w_0^3\right) + \mathcal{O}(w_0^4)\,, \tag{5.7}$$

where the c_i are irreducible polynomials in a_i and b_i. This implies that the discriminant $\Delta = 4f^3 + 27g^2$ takes the form

$$\Delta = \frac{1}{16}\left(a_{10}^4 \cdot b_1^4 \cdot a_{11} \cdot b_2 \cdot b_3 \cdot c_5 \cdot c_6 \cdot c_7 \cdot w_0^5 + a_{10}^2 \cdot b_1^2 \cdot c_8 \cdot w_0^6 + c_9 \cdot w_0^7\right) + \mathcal{O}(w_0^8) \tag{5.8}$$

with

$$c_5 = a_{10}a_{12}b_1^2 - a_9a_{10}b_1b_3 + a_6a_{11}b_1b_3 + a_3a_{10}b_3^2 \tag{5.9}$$

$$c_6 = -a_8a_{10}b_1^2 + a_5a_{11}b_1^2 + a_7a_{10}b_1b_2 - a_4a_{11}b_1b_2 + a_3a_{11}b_2^2 \tag{5.10}$$

$$\begin{aligned} c_7 = {} & a_3a_{10}^2b_0^2 + a_4a_6a_{10}b_0b_1 - a_1a_{10}^2b_0b_1 + a_5a_6^2b_1^2 - a_2a_6a_{10}b_1^2 + a_0a_{10}^2b_1^2 \\ & - 2a_3a_6a_{10}b_0b_2 - a_4a_6^2b_1b_2 + a_1a_6a_{10}b_1b_2 + a_3a_6^2b_2^2\,. \end{aligned} \tag{5.11}$$

From the vanishing orders of the f, g and Δ we observe that there are seven distinct matter curves and list them in Table 6.

Name	Equation	Singularity type	$SU(5)$ representation
T_1	$a_{10} \cap w_0$	$SO(10)$	**10**
T_2	$b_1 \cap w_0$	$SO(10)$	**10**
F_1	$a_{11} \cap w_0$	$SU(7)$	**5**
F_2	$b_2 \cap w_0$	$SU(7)$	**5**
F_3	$c_5 \cap w_0$	$SU(7)$	**5**
F_4	$c_6 \cap w_0$	$SU(7)$	**5**
F_5	$c_7 \cap w_0$	$SU(7)$	**5**
F_6	$b_3 \cap w_0$	$SU(7)$	**5**

Table 6: *The matter curves for the top of Table 5.*

While the appearance of two different **10** curves and six distinct **5** curves is promising, it is crucial to check which of these curves are actually realized in a generic fibration of this top over a base manifold. Next, we therefore fiber this space over a $\mathbb{P}^3$. Doing so can be achieved by embedding the rays of Table 4 into $\mathbb{Z}^6$ according to

$$v_i \mapsto u_i \equiv (v_i, 0, 0, 0), \qquad i = 1, \ldots, 5\,, \tag{5.12}$$

adding the blowup rays from Table 5 with $w_0 = (1, 0, 0)$ and adding the remaining 3 base rays:

$$u_7 = (0, 0, 0, -1, -1, -1)\ , \quad u_8 = (n_1, n_2, n_3, 0, 1, 0)\ , \quad u_9 = (0, 0, 0, 0, 0, 1)\ . \tag{5.13}$$

Here the n_i are integers encoding the fibration of the fiber over the base. More specifically, the n_i determine which line bundles the fiber coordinates are sections of. For our purposes, we choose $(n_1, n_2, n_3) = (-1, 0, 0)$. After using PALP to compute all nef partitions of the resulting polytope, we pick the one with

$$\nabla_1 = \langle u_1, u_2, u_3, u_4, u_5, u_6, u_7, u_8, e_0, e_1, e_2\rangle_{\text{conv}}\,, \qquad \nabla_2 = \langle u_0, e_3, e_4\rangle_{\text{conv}}\,. \tag{5.14}$$

It has Hodge numbers $h^{1,1} = 8$, $h^{2,1} = 0$, and $h^{3,1} = 141$. For this specific choice of fibration, both b_0 and b_3 are constants. Consequently, the curve F_6 is not realized. However, all other curves *exist* and in particular, there are two different antisymmetric representations. Using the

Singularity type	Coupling	Multiplicity
$SU(7)$	$\mathbf{5}_{(4,3)} \times \overline{\mathbf{5}}_{(1,2)}$	54
$SU(7)$	$\mathbf{5}_{(-1,3)} \times \overline{\mathbf{5}}_{(1,2)}$	39
$SU(7)$	$\mathbf{5}_{(-1,3)} \times \overline{\mathbf{5}}_{(-4,-3)}$	36
$SU(7)$	$\mathbf{5}_{(-6,-7)} \times \overline{\mathbf{5}}_{(1,2)}$	27
$SU(7)$	$\mathbf{5}_{(-6,-7)} \times \overline{\mathbf{5}}_{(-4,-3)}$	12
$SU(7)$	$\mathbf{5}_{(-6,-7)} \times \overline{\mathbf{5}}_{(1,-3)}$	9
$SU(7)$	$\mathbf{5}_{(-6,-2)} \times \overline{\mathbf{5}}_{(1,2)}$	9
$SU(7)$	$\mathbf{5}_{(-6,-2)} \times \overline{\mathbf{5}}_{(-4,-3)}$	6
$SU(7)$	$F\mathbf{5}_{(-6,-2)} \times \overline{\mathbf{5}}_{(1,-3)}$	6
$SU(7)$	$\mathbf{5}_{(-6,-7)} \times \overline{\mathbf{5}}_{(6,2)}$	3
$SO(12)$	$\overline{\mathbf{10}}_{(-3,-1)} \times \mathbf{5}_{(4,3)} \times \mathbf{5}_{(-1,-2)}$	15
$SO(12)$	$\overline{\mathbf{10}}_{(2,4)} \times \mathbf{5}_{(-1,-2)} \times \mathbf{5}_{(-1,-2)}$	3
$SO(12)$	$\overline{\mathbf{10}}_{(2,4)} \times \mathbf{5}_{(-6,-2)} \times \mathbf{5}_{(4,3)}$	3
E_6	$\mathbf{10}_{(3,1)} \times \mathbf{10}_{(3,1)} \times \mathbf{5}_{(-6,-2)}$	3
E_6	$\mathbf{10}_{(3,1)} \times \mathbf{10}_{(-2,-4)} \times \mathbf{5}_{(-1,3)}$	3

Table 7: *All couplings involving multiple non-Abelian matter representations in the example of Equation 5.13. Note that there are additional non-minimal singularities that do not list here.*

Chern-Simons matching as in [9, 45, 46], we find that the realized curves have the following charges under the two $U(1)$s:

$$T_1 : \ \mathbf{10}_{(3,1)} \,, \qquad T_2 : \ \mathbf{10}_{(-2,-4)} \tag{5.15}$$

$$F_1 : \ \mathbf{5}_{(-6,-7)} \,, \quad F_2 : \ \mathbf{5}_{(-6,-2)} \,, \quad F_3 : \ \mathbf{5}_{(-1,3)} \,, \quad F_4 : \ \mathbf{5}_{(4,3)} \,, \quad F_5 : \ \mathbf{5}_{(-1,-2)} \tag{5.16}$$

We also find the following singlet states:

$$\mathbf{1}_{(5,0)} \,, \quad \mathbf{1}_{(0,5)} \,, \quad \mathbf{1}_{(5,5)} \,, \quad \mathbf{1}_{(5,10)} \,, \quad \mathbf{1}_{(10,5)} \,, \quad \mathbf{1}_{(10,10)} \,. \tag{5.17}$$

Finally, we compute the Yukawa couplings for the given example and find the ones listed in Table 7.

In summary, we have managed to construct a fully explicit F-theory model with gauge group $SU(5) \times U(1)^2$, in which the *torically realized* $SU(5)$ singularity gives rise to a gauge theory with two different **10** representations. Clearly the example studied here is not intended to be used as a full-fledged GUT model. In more realistic models several issues would need to be addressed, such as the fact that there exist non-minimal singularities at points in the base manifold whose resolution leads to a non-flat fibration. Furthermore, the topology of the GUT divisor is too simple in order to allow hypercharge flux with the desired properties. In principle, both these points can be addressed by choosing the fibration more carefully than we did following equation (5.13).

5.2 $SU(5) \times U(1)^2$ and a Discrete Symmetry

The second example we consider is a nef partition of the polytope with the least integral points, that is the one corresponding to $\mathbb{P}^3$. Its polytope is of course well-known, but for completeness we list it in Table 8. All toric divisors $V(z_i)$ inside $\mathbb{P}^3$ lie in the same homology class and

v_0	v_1	v_2	v_3
$\begin{pmatrix}-1\\-1\\-1\end{pmatrix}$	$\begin{pmatrix}0\\0\\1\end{pmatrix}$	$\begin{pmatrix}0\\1\\0\end{pmatrix}$	$\begin{pmatrix}1\\0\\0\end{pmatrix}$

Table 8: *Vertices of the reflexive polytope corresponding to $\mathbb{P}^3$. Since it has the least integral points of all reflexive polytopes in three dimensions, it has PALP id 0.*

therefore it can only have two nef partitions: The one corresponding to a partition of $3+1$ vertices and the nef partition corresponding to a partition of $2+2$ vertices. The first is again a projection and to have some variety, we therefore focus on the latter. That is, we take our nef partition to be

$$\nabla_1 = \langle v_0, v_3 \rangle_{\text{conv}}\,, \qquad \nabla_2 = \langle v_1, v_2 \rangle_{\text{conv}}\,. \tag{5.18}$$

This implies automatically that all toric divisors intersect a generic complete intersection of this type in four points:

$$V(z_i) \cap E = \int_E [V(z_i)] = \int_{\mathbb{P}^3} [2H]\cdot[2H]\cdot[H] = 4\,. \tag{5.19}$$

A generic fibration with this fiber will therefore not have a section. As noted in the introduction, F-theory models without section have recently received quite some attention, see [2, 17–21]. However, in these models the Calabi-Yau manifolds always had 2- or 3-sections leading to $\mathbb{Z}_2$ or $\mathbb{Z}_3$ discrete gauge symmetries, respectively. As the biquadric in $\mathbb{P}^3$ has a 4-section, we expect to find a discrete $\mathbb{Z}_4$ gauge group. In the following we will try to collect some further evidence for this.

To do, let us take the same approach as with the previous example and write down the defining equations of the complete intersection. They read

$$\begin{aligned} p_1 &= \tilde{a}_0 z_0^2 + \tilde{a}_1 z_0 z_1 + \tilde{a}_2 z_1^2 + \tilde{a}_3 z_0 z_2 + \tilde{a}_4 z_1 z_2 + \tilde{a}_5 z_2^2 + \tilde{a}_6 z_0 z_3 + \tilde{a}_7 z_1 z_3 + \tilde{a}_8 z_2 z_3 + \tilde{a}_9 z_3^2 \\ p_2 &= \tilde{b}_0 z_0^2 + \tilde{b}_1 z_0 z_1 + \tilde{b}_2 z_1^2 + \tilde{b}_3 z_0 z_2 + \tilde{b}_4 z_1 z_2 + \tilde{b}_5 z_2^2 + \tilde{b}_6 z_0 z_3 + \tilde{b}_7 z_1 z_3 + \tilde{b}_8 z_2 z_3 + \tilde{b}_9 z_3^2\,. \end{aligned} \tag{5.20}$$

Note that such biquadrics have been studied before in [47] and, with the restriction to the triple blowup of $\mathbb{P}^3$, in [15]. Since this nef partition is not a projection, one cannot bring this complete intersection into Weierstrass form by solving one of the equations for one variable and substituting the result into the other equation.

Next, we tune the $\tilde{a}_i$ and $\tilde{b}_i$ such as to enforce an $SU(5)$ singularity along the divisor $e_0 = 0$ in the base manifold. Then we resolve this singularity by introducing exceptional divisors e_i,

e_0	e_1	e_2	e_3	e_4
$\begin{pmatrix}0\\0\\0\\w_0\end{pmatrix}$	$\begin{pmatrix}-1\\-1\\-1\\w_0\end{pmatrix}$	$\begin{pmatrix}-1\\-1\\0\\w_0\end{pmatrix}$	$\begin{pmatrix}0\\-1\\0\\w_0\end{pmatrix}$	$\begin{pmatrix}0\\-1\\-1\\w_0\end{pmatrix}$

Table 9: *As before, the blowup of equations (5.21) and (5.22) corresponds to introducing the top defined here, where w_0 is a ray of the fan of the base. The GUT brane will then be located on the divisor corresponding to w_0. We again denote rays and corresponding homogeneous variables by the same letters.*

$i = 1, \ldots, 4$ as specified torically in terms of the top of Table 9. We find that the coefficients $\tilde{a}_i$ and $\tilde{b}_i$ take the form

$$\begin{aligned}
&\tilde{a}_0 = a_0 \cdot e_1^2 e_2^2 e_3 e_4 && \tilde{a}_1 = a_1 \cdot e_1 e_2^2 e_3 && \tilde{a}_2 = a_2 \cdot e_0 e_1 e_2^3 e_3^2 \\
&\tilde{a}_3 = a_3 \cdot e_1 e_2 && \tilde{a}_4 = a_4 \cdot e_0 e_1 e_2^2 e_3 && \tilde{a}_5 = a_5 \cdot e_0 e_1 e_2 \\
&\tilde{a}_6 = a_6 \cdot e_1 e_2 e_3 e_4 && \tilde{a}_7 = a_7 \cdot e_2 e_3 && \tilde{a}_8 = a_8 \\
& && \tilde{a}_9 = a_9 \cdot e_3 e_4 &&
\end{aligned} \tag{5.21}$$

and

$$\begin{aligned}
&\tilde{b}_0 = b_0 \cdot e_1 e_4 && \tilde{b}_1 = b_1 && \tilde{b}_2 = b_2 \cdot e_0 e_2 e_3 \\
&\tilde{b}_3 = b_3 \cdot e_0 e_1 e_4 && \tilde{b}_4 = b_4 \cdot e_0 && \tilde{b}_5 = b_5 \cdot e_0^2 e_1 e_4 \\
&\tilde{b}_6 = b_6 \cdot e_0 e_1 e_3 e_4^2 && \tilde{b}_7 = b_7 \cdot e_0 e_3 e_4 && \tilde{b}_8 = b_8 \cdot e_0^2 e_1 e_3 e_4^2 \\
& && \tilde{b}_9 = b_9 \cdot e_0^2 e_1 e_3^2 e_4^3 \,. &&
\end{aligned} \tag{5.22}$$

Here a_i and b_i are polynomials in the base variables that depend on e_i only through the combination $w_0 \equiv e_0 e_1 e_2 e_3 e_4$. As a power series in w_0, the Weierstrass coefficients read

$$f = -\frac{1}{768}\Big(a_8^4 \cdot b_1^4 + 2 \cdot a_8^2 \cdot b_1^2 \cdot c_1 \cdot w_0 + c_2 \cdot w_0^2\Big) + \mathcal{O}(w_0^3) \tag{5.23}$$

$$g = \frac{1}{55296}\Big(a_8^6 \cdot b_1^6 - 3 \cdot a_8^4 \cdot b_1^4 \cdot c_1 \cdot w_0 + a_8^2 \cdot b_1^2 \cdot c_3 \cdot w_0^2 + c_4 \cdot w_0^3\Big) + \mathcal{O}(w_0^4)\,, \tag{5.24}$$

where the c_i are irreducible polynomials in a_i and b_i. Then the discriminant is

$$\Delta = \frac{1}{2^{16}}\Big(a_8^4 \cdot b_1^4 \cdot c_5 \cdot c_6 \cdot c_7 \cdot c_8 \cdot w_0^5 + a_8^2 \cdot b_1^2 \cdot c_9 \cdot v_0^6 + c_{10} \cdot w_0^7\Big) + \mathcal{O}(w_0^8) \tag{5.25}$$

with

$$c_5 = -b_1 b_3 b_4 + b_0 b_4^2 + b_1^2 b_5 \tag{5.26}$$

$$c_6 = a_3 a_7 a_8 b_0 - a_1 a_8^2 b_0 - a_3 a_6 a_8 b_1 + a_0 a_8^2 b_1 + a_3^2 a_9 b_1 \tag{5.27}$$

$$c_7 = -a_5 a_7^2 b_1 + a_4 a_7 a_8 b_1 - a_2 a_8^2 b_1 - a_3 a_7 a_8 b_2 + a_1 a_8^2 b_2 + a_3 a_7^2 b_4 - a_1 a_7 a_8 b_4 \tag{5.28}$$

$$\begin{aligned}
c_8 = &-a_9^2 b_1 b_3 b_4 + a_9^2 b_0 b_4^2 + a_9^2 b_1^2 b_5 + a_8 a_9 b_1 b_4 b_6 + a_8 a_9 b_1 b_3 b_7 - 2 a_8 a_9 b_0 b_4 b_7 \\
&- a_8^2 b_1 b_6 b_7 + a_8^2 b_0 b_7^2 - a_8 a_9 b_1^2 b_8 + a_8^2 b_1^2 b_9\,.
\end{aligned} \tag{5.29}$$

We observe that there are six distinct matter curves and list them in Table 10. This by itself is another piece of evidence that there exists in fact an order 4 discrete symmetry. Arguing along the lines of [20, 21], it is this symmetry that helps to distinguish the four **5** representations that would otherwise have identical quantum numbers in the low-energy effective action.

Name	Equation	Singularity type	$SU(5)$ representation
T_1	$a_8 \cap w_0$	$SO(10)$	**10**
T_2	$b_1 \cap w_0$	$SO(10)$	**10**
F_1	$c_5 \cap w_0$	$SU(7)$	**5**
F_2	$c_6 \cap w_0$	$SU(7)$	**5**
F_3	$c_7 \cap w_0$	$SU(7)$	**5**
F_4	$c_8 \cap w_0$	$SU(7)$	**5**

Table 10: *The matter curves in the example with the elliptic fiber embedded as a biquadric in $\mathbb{P}^3$.*

Singularity type	Coupling	Multiplicity
$SU(7)$	$F_1 \times F_2$	30
$SU(7)$	$F_1 \times F_3$	42
$SU(7)$	$F_1 \times F_4$	36
$SU(7)$	$F_2 \times F_3$	33
$SU(7)$	$F_2 \times F_4$	40
$SU(7)$	$F_3 \times F_4$	56
$SO(12)$	$T_1 \times F_1 \times F_4$	6
$SO(12)$	$T_1 \times F_2 \times F_2$	1
$SO(12)$	$T_1 \times F_3 \times F_3$	2
$SO(12)$	$T_2 \times F_1 \times F_1$	6
$SO(12)$	$T_2 \times F_2 \times F_3$	9
$SO(12)$	$T_2 \times F_4 \times F_4$	9
E_6	$T_1 \times T_1 \times F_3$	3
E_6	$T_1 \times T_2 \times F_2$	3
E_6	$T_2 \times T_2 \times F_3$	12

Table 11: *All couplings involving multiple non-Abelian matter representations in the example with the elliptic fiber embedded in $\mathbb{P}^3$. Note that there are additional non-minimal singularities that do not list here.*

As before, we can make this more concrete by constructing an explicit example. To do so, we use the same embedding into $\mathbb{Z}^6$ as in equation (5.13), but this time we set $(n_1, n_2, n_3) = (0, 0, 1)$ and denote the rays obtained by embedding the base divisors w_i, $i = 1, 2, 3$ by u_5, u_6, and u_7. The resulting six-dimensional lattice polytope has 33 nef partitions. Of these, let us pick the

nef partition

$$\nabla_1 = \langle u_0, u_3, u_5, e_1, e_2, e_3, e_4 \rangle_{\text{conv}} \,, \qquad \nabla_2 = \langle u_1, u_2, e_0, u_6, u_7 \rangle_{\text{conv}} \,, \tag{5.30}$$

which has the Hodge numbers $h^{1,1} = 6$, $h^{2,1} = 0$, and $h^{3,1} = 110$. For this explicit example, we find that all the curves listed in Table 10 are in fact realized geometrically. In Table 11 we furthermore list the Yukawa points involving multiple non-Abelian representations. Since Yukawa couplings must be invariant under gauge symmetries, the couplings that do not involve singlets allow us to determine the $\mathbb{Z}_4$ charges of the six matter curves. Let us denote the neutral element of $\mathbb{Z}_4$ by 0 and call the generator e. Then we have that the two couplings involving only T_1 and F_3 imply

$$2 \cdot Q_{\mathbb{Z}_4}(T_1) + Q_{\mathbb{Z}_4}(F_3) = 0 \,, \qquad 2 \cdot Q_{\mathbb{Z}_4}(F_3) = T_1 \tag{5.31}$$

which immediately leads to

$$Q_{\mathbb{Z}_4}(T_1) = Q_{\mathbb{Z}_4}(F_3) = 0 \,. \tag{5.32}$$

The remaining couplings then imply that

$$Q_{\mathbb{Z}_4}(F_2) = Q_{\mathbb{Z}_4}(T_2) = 2e \,. \tag{5.33}$$

Last but not least, we have $Q_{\mathbb{Z}_4}(F_{1/4}) \in \{e, 3e\}$. However, e and $3e$ are the only order 4 elements of $\mathbb{Z}_4$ and we could just as well take $e' = 3e$ as the generator of $\mathbb{Z}_4$. As a consequence, one can simply choose that

$$Q_{\mathbb{Z}_4}(F_1) = e \,, \qquad Q_{\mathbb{Z}_4}(F_4) = 3e \,. \tag{5.34}$$

With these charge assignments one finds that singlets with all allowed $\mathbb{Z}_4$ charges must be present in order to make all the couplings of Table 11 invariant.

Put in a nutshell, we find that one can easily realize F-theory models with a non-Abelian gauge group accompanied solely by an additional discrete symmetry of order 4. A convenient way of doing so proceeds by embedding the elliptic fiber as a biquadric inside $\mathbb{P}^3$. There are numerous ways of extending the treatment here, such as connecting this model to others in terms of Higgsings and conifold transitions in the circle-compactified theories.

5.3 Example with Mordell-Weil Torsion $\mathbb{Z}_4$

As a final example, let us take a quick look at a model with Mordell-Weil torsion $\mathbb{Z}_4$. This torsion group does not exist generically for codimension one elliptic fibers [16, 17, 48] and even in codimension two there is only a single example as can be seen from Table 3.

Mordell-Weil torsion was studied extensively in [48] and it was found that it impacts the global structure of the non-Abelian gauge group. Given a singularity of type A_{n-1}, the universal covering group is $SU(n)$, which, without Mordell-Weil torsion, constitutes the gauge group of

the F-theory model. In the presence of a non-trivial Mordell-Weil torsion group $\mathbb{Z}_k$ this changes: The non-Abelian gauge group becomes $SU(n)/\mathbb{Z}_k$. By construction the universal covering group has a trivial first fundamental group, and therefore the effect of non-trivial Mordell-Weil torsion is that the non-Abelian gauge group of the low-energy effective theory is no longer simply connected:

$$\pi_1(SU(n)/\mathbb{Z}_k) = \mathbb{Z}_k\,. \tag{5.35}$$

In the examples studied in [48] Mordell-Weil torsion groups $\mathbb{Z}_2$ and $\mathbb{Z}_3$ always came accompanied by gauge groups of type $SU(2n)$ and $SU(3n)$, respectively. Since $SU(n)$ has a $\mathbb{Z}_n$ center generated by the identity matrix times $e^{\frac{2\pi i}{n}}$, one can mod out $\mathbb{Z}_k$ by eliminating the center (or a subgroup thereof) of $SU(k\cdot n)$.

v_0	v_1	v_2	v_3	v_4	v_5	v_6	v_7
$\begin{pmatrix}1\\0\\0\end{pmatrix}$	$\begin{pmatrix}0\\1\\0\end{pmatrix}$	$\begin{pmatrix}1\\-1\\0\end{pmatrix}$	$\begin{pmatrix}-1\\0\\0\end{pmatrix}$	$\begin{pmatrix}0\\1\\2\end{pmatrix}$	$\begin{pmatrix}-1\\0\\-2\end{pmatrix}$	$\begin{pmatrix}-1\\-2\\-2\end{pmatrix}$	$\begin{pmatrix}2\\1\\2\end{pmatrix}$

Table 12: *Vertices of the three-dimensional reflexive polytope with PALP id* 3415.

The corresponding reflexive polytope has PALP id 3415 and we list its defining data in Table 12. It has a single nef partition, namely

$$\nabla_1 = \langle v_0, v_3, v_5, v_6\rangle_{\text{conv}}\,, \qquad \nabla_2 = \langle v_1, v_2, v_4, v_7\rangle_{\text{conv}}\,. \tag{5.36}$$

In order to write down the most general complete intersection corresponding to this nef partition, we must use every integral point of the polytope defined in Table 12 apart from the origin. The additional eleven points are listed in Table 13.

After resolution, the complete intersection defined by (5.36) is defined by the following two polynomials:

$$\begin{aligned} p_1 &= a_0 z_0 z_3 z_5 z_6 z_8 z_{10} z_{12} z_{15} z_{17} + a_1 z_0^2 z_7^2 z_8 z_9 z_{14} z_{15} z_{16} + a_2 z_3^2 z_4^2 z_{10} z_{11} z_{14} z_{17} z_{18} \\ p_2 &= b_0 z_1^2 z_5^2 z_{12} z_{15} z_{16} z_{17} z_{18} + b_1 z_2^2 z_6^2 z_8 z_9 z_{10} z_{11} z_{12} + b_2 z_1 z_2 z_4 z_7 z_9 z_{11} z_{14} z_{16} z_{18}\,. \end{aligned} \tag{5.37}$$

v_8	v_9	v_{10}	v_{11}	v_{12}	v_{13}	v_{14}	v_{15}	v_{16}	v_{17}	v_{18}
$\begin{pmatrix}0\\-1\\-1\end{pmatrix}$	$\begin{pmatrix}1\\0\\1\end{pmatrix}$	$\begin{pmatrix}-1\\-1\\-1\end{pmatrix}$	$\begin{pmatrix}0\\0\\1\end{pmatrix}$	$\begin{pmatrix}-1\\-1\\-2\end{pmatrix}$	$\begin{pmatrix}0\\0\\0\end{pmatrix}$	$\begin{pmatrix}1\\1\\2\end{pmatrix}$	$\begin{pmatrix}0\\0\\-1\end{pmatrix}$	$\begin{pmatrix}1\\1\\1\end{pmatrix}$	$\begin{pmatrix}-1\\0\\-1\end{pmatrix}$	$\begin{pmatrix}0\\1\\1\end{pmatrix}$

Table 13: *Integral points of the reflexive polytope with PALP id* 3415 *that are neither vertices nor the origin. In order to fully resolve every fibration of the nef partition* (5.36) *one must use all of these points as rays of the toric fan.*

This time we are not interested in engineering additional singularities, but rather in confirming that models with this fiber contain the $SU(4)$ gauge factors that we expect to exist. To this end we compute the discriminant of the elliptic curve and find

$$f = -\frac{1}{48} \cdot \left(16a_1^2a_2^2b_0^2b_1^2 - 16a_0^2a_1a_2b_0b_1b_2^2 + a_0^4b_2^4\right) \tag{5.38}$$

$$g = \frac{1}{864} \cdot \left(8a_1a_2b_0b_1 - a_0^2b_2^2\right) \cdot \left(8a_1^2a_2^2b_0^2b_1^2 + 16a_0^2a_1a_2b_0b_1b_2^2 - a_0^4b_2^4\right) \tag{5.39}$$

$$\Delta = -\frac{1}{16} \cdot a_0^2 \cdot b_2^2 \cdot a_1^4 \cdot a_2^4 \cdot b_0^4 \cdot b_1^4 \cdot \left(-16a_1a_2b_0b_1 + a_0^2b_2^2\right) \ . \tag{5.40}$$

From the vanishing orders we see that there are two I_2 and four I_4 singularities. Since

$$\left.\frac{9g}{2f}\right|_{a_1=0} = \left.\frac{9g}{2f}\right|_{a_2=0} = \left.\frac{9g}{2f}\right|_{b_1=0} = \left.\frac{9g}{2f}\right|_{b_2=0} = -\frac{1}{4}a_0^2b_3^2 \tag{5.41}$$

the I_4 singularities are of split type (see [49] or Appendix A) and we therefore see that there is indeed a non-toric $SU(2)^2 \times SU(4)^4/\mathbb{Z}_4$ gauge group. One can mod out the $\mathbb{Z}_4$ torsion by identifying it with the diagonal subgroup of the center $\mathbb{Z}_4^{\oplus 4}$ of the $SU(4)$ gauge group part.

It is interesting to see that up to a lattice isomorphism the reflexive polytope ∇° associated to the nef partition (5.36) is precisely the polytope with PALP id 0. Under the same lattice isomorphism, the Δ_i of (5.36) are mapped to the ∇_i of (5.18) and we therefore see that the fiber considered in this subsection is mirror-dual to the fiber of Subsection 5.2. In particular, it appears that under this duality the discrete gauge group part is mapped to the torsion part of the Mordell-Weil group and vice versa. The same behavior was observed in [17] for hypersurface fibers and it is intriguing to speculate about a possible physical reason underlying this observation.

Finally, let us note that it would be interesting to study explicit realizations of such fibrations. While this is possible in principle, the large number of involved points might make it technically challenging to find a triangulation that gives rise to an appropriate toric fan of the ambient variety. In the recent work [50] it was used that the relevant triangulations are star triangulations with respect to the origin in order to speed up the calculation. It would exciting to incorporate such an algorithm in the Sage software package and apply it to these spaces.

6 Conclusions

In this paper we proposed a new algorithm to bring a large class of elliptic curves as well as the Jacobians of genus-one curves into Weierstrass form. The essential step of this algorithm is to obtain an appropriate line bundle whose sections can be used as coordinates for an embedding into either $\mathbb{P}_{231}$, $\mathbb{P}_{112}$, $\mathbb{P}^2$, or $\mathbb{P}^3$. While it is not always possible to identify such a line bundle, the class for which this can be achieved is much larger than the class of models that one has so far been able to bring into Weierstrass form. To illustrate this fact, we computed the Weierstrass forms of all nef partitions of three-dimensional reflexive polytopes that do not correspond to

product spaces, which allowed us to compute the toric Mordell-Weil group of all 3134 complete intersection curves of codimension two. Compared to the analogous analysis for hypersurfaces [16], we find additional groups, such as a free Abelian group of rank four or the pure torsion group $\mathbb{Z}_4$. Additionally, we computed the non-toric non-Abelian gauge groups and again found a considerably larger variety of than those that were encountered in [17] for hypersurface fibers.

In Section 5 we proceeded by selecting three particular examples that exhibit features that are ruled out for hypersurface fibers. These are torically realized $SU(5)$ models whose antisymmetric representations have different charges under the additional Abelian factors, models with a discrete $\mathbb{Z}_4$ symmetry and, finally, F-theory models with a $\mathbb{Z}_4$ torsion factor. For the first two types we give an explicit toric realization with non-Abelian gauge group $SU(5)$ and determine the matter curves that are present as well as the Yukawa couplings that the non-Abelian representations are involved in.

There are numerous exciting ways in which this work could be extended in the future. On the one hand, there are systematic questions that one could address, such as a classification of higher-dimensional tops encoding the toric gauge groups or the construction of all fibrations with a given top. For hypersurfaces these questions have already been answered in [44] and [16], respectively, but it would be interesting to see how these result generalize to higher codimensions. On the other hand, one could use the methods developed here in order to construct explicit scenarios for studying new physical effects. Section 5 dealt with some potentially interesting set-ups, but naturally there exist many more. Viewed more generally, one could hope that access to a large number of fiber types might allow one to make observations about the landscape of F-theory models [51–54]. In [17] such observations were made based on the results for the 16 hypersurface fibers and, for instance, a network of Higgsing transitions was found. Given the much larger number of models studied here might allow to find even deeper relations between seemingly different fiber types.

Acknowledgments

We would like to thank Philip Candelas, Iñaki García-Etxebarria, and Tom Pugh for interesting discussions. The work of T.G. and J.K. is supported by a grant of the Max Planck Society. V.B. is supported by the EPSRC grant BKRWDM00.

A List of Non-Toric Non-Abelian Gauge Groups

In this appendix we list the non-toric non-Abelian gauge groups that are present if the coefficients a_i defining the complete intersection are chosen generically. In order to determine these singularities we computed the Weierstrass forms of the genus-one curves and factorized f, g and Δ. The vanishing degrees along an irreducible factor then determine the singularity over the vanishing locus of that factor. We quote Table 14 from [49] for a dictionary to translate the

vanishing degrees into the Kodaira type. Since the total number of singularities we find is very large, we have split up our results into tables 15, 16, 17 and 18. Note that we do not include the disconnected spaces corresponding to direct product nef partitions.

	$\mathrm{ord}_\Sigma(f)$	$\mathrm{ord}_\Sigma(g)$	$\mathrm{ord}_\Sigma(\Delta)$	Eqn. of monodromy cover	$\mathfrak{g}(\Sigma)$
I_2	0	0	2	–	$\mathfrak{su}(2)$
I_m, $m \geq 3$	0	0	m	$\psi^2 + (9g/2f)\|_{z=0}$	$\mathfrak{sp}(\lceil \frac{m}{2} \rceil)$ or $\mathfrak{su}(m)$
I_0^*	≥ 2	≥ 3	6	$\psi^3 + (f/z^2)\|_{z=0} \cdot \psi + (g/z^3)\|_{z=0}$	$\mathfrak{g}_2$ or $\mathfrak{so}(7)$ or $\mathfrak{so}(8)$
I_{2n-5}^*, $n \geq 3$	2	3	$2n+1$	$\psi^2 + \frac{1}{4}(\Delta/z^{2n+1})(2zf/9g)^3\|_{z=0}$	$\mathfrak{so}(4n-3)$ or $\mathfrak{so}(4n-2)$
I_{2n-4}^*, $n \geq 3$	2	3	$2n+2$	$\psi^2 + (\Delta/z^{2n+2})(2zf/9g)^2\|_{z=0}$	$\mathfrak{so}(4n-1)$ or $\mathfrak{so}(4n)$
IV^*	≥ 3	4	8	$\psi^2 - (g/z^4)\|_{z=0}$	$\mathfrak{f}_4$ or $\mathfrak{e}_6$
III^*	3	≥ 5	9	–	$\mathfrak{e}_7$
II^*	≥ 4	5	10	–	$\mathfrak{e}_8$

Table 14: *Kodaira–Tate classification of singular fibers, monodromy covers, and gauge algebras, taken from [49]. The column with the gauge algebras is to be understood as follows: Assume that the defining equation of the monodromy cover splits into n irreducible pieces. Then the resulting gauge algebra is the n^{th} algebra listed in the last column.*

Generic non-toric Kodaira singularities	Occurences
No singularity	88
IV^*	3
$IV^* \times I_2$	8
$IV^* \times I_2 \times I_3$	9
$IV^* \times I_2^2$	4
$IV^* \times I_2^2 \times I_3$	4
$IV^* \times I_2^3 \times I_3$	1
$IV^* \times I_3^3$	1
$IV^* \times I_3^4$	1
$III^* \times I_2$	2
$III^* \times I_2 \times I_3$	4
$III^* \times I_2^2$	1
$III^* \times I_2^2 \times I_4$	1
$III^* \times I_2^3 \times I_4$	1
$II^* \times I_2 \times I_3$	1

Table 15: *List of generic non-toric E- and F_4-type Kodaira singularities and the number of times they occur.*

Generic non-toric Kodaira singularities	Occurences
I_0^*	39
$I_0^* \times I_2$	47
$I_0^* \times I_2 \times I_3$	15
$I_0^* \times I_2 \times I_3^2$	4
$I_0^* \times I_2^2$	27
$I_0^* \times I_2^2 \times I_3$	17
$I_0^* \times I_2^2 \times I_4$	5
$I_0^* \times I_2^2 \times I_4^2$	4
$I_0^* \times I_2^3$	15
$I_0^* \times I_2^3 \times I_4$	4
$I_0^* \times I_2^4$	2
$I_0^* \times I_2^4 \times I_4$	3
$I_0^* \times I_2^5$	2
I_1^*	9
$I_1^* \times I_2$	20
$I_1^* \times I_2 \times I_3$	9
$I_1^* \times I_2^2$	13
$I_1^* \times I_2^2 \times I_3$	8
$I_1^* \times I_2^2 \times I_3^2$	2
$I_1^* \times I_2^3$	4
$I_1^* \times I_2^3 \times I_3$	2
$I_2^* \times I_2$	3
$I_2^* \times I_2 \times I_3$	7
$I_2^* \times I_2^2$	5
$I_2^* \times I_2^2 \times I_4$	2
$I_2^* \times I_2^3 \times I_4$	2
$I_2^* \times I_2^4$	1
$I_2^* \times I_2^5$	1
$I_3^* \times I_2 \times I_3$	2
$I_3^* \times I_2^2 \times I_3$	1
$I_4^* \times I_2^2 \times I_4$	1

Table 16: *List of generic non-toric G_2 and SO-type Kodaira singularities and the number of times they occur.*

Generic non-toric Kodaira singularities	Occurences
I_2	263
$I_2 \times I_3$	141
$I_2 \times I_3 \times I_4$	41
$I_2 \times I_3 \times I_5$	12
$I_2 \times I_3 \times I_6$	32
$I_2 \times I_3 \times I_7$	6
$I_2 \times I_3^2$	41
$I_2 \times I_3^2 \times I_4$	15
$I_2 \times I_3^3$	13
$I_2 \times I_4$	136
$I_2 \times I_4^2$	4
$I_2 \times I_4^4$	1
$I_2 \times I_5$	26
$I_2 \times I_6$	6
I_2^2	326
$I_2^2 \times I_3$	170
$I_2^2 \times I_3 \times I_4$	69
$I_2^2 \times I_3 \times I_5$	14
$I_2^2 \times I_3 \times I_6$	12
$I_2^2 \times I_3 \times I_7$	4
$I_2^2 \times I_3 \times I_8$	2
$I_2^2 \times I_3^2$	54
$I_2^2 \times I_3^2 \times I_4$	15
$I_2^2 \times I_3^2 \times I_5$	6
$I_2^2 \times I_3^3$	3
$I_2^2 \times I_3^3 \times I_4$	2
$I_2^2 \times I_4$	134
$I_2^2 \times I_4 \times I_6$	6
$I_2^2 \times I_4 \times I_8$	8
$I_2^2 \times I_4^2$	27
$I_2^2 \times I_4^3$	12
$I_2^2 \times I_4^4$	1
$I_2^2 \times I_5$	28
$I_2^2 \times I_6$	22
$I_2^2 \times I_7$	2

Table 17: *List of generic non-toric Sp and SU-type Kodaira singularities and the number of times they occur, part I.*

Generic non-toric Kodaira singularities	Occurences
I_2^3	260
$I_2^3 \times I_3$	121
$I_2^3 \times I_3 \times I_4$	24
$I_2^3 \times I_3 \times I_5$	4
$I_2^3 \times I_3 \times I_6$	4
$I_2^3 \times I_3^2$	16
$I_2^3 \times I_4$	85
$I_2^3 \times I_4 \times I_6$	6
$I_2^3 \times I_4^2$	10
$I_2^3 \times I_5$	10
I_2^4	133
$I_2^4 \times I_3$	30
$I_2^4 \times I_3 \times I_4$	2
$I_2^4 \times I_3^2$	4
$I_2^4 \times I_4$	29
$I_2^4 \times I_4^2$	10
$I_2^4 \times I_5$	2
$I_2^4 \times I_6$	4
$I_2^4 \times I_8$	2
I_2^5	32
$I_2^5 \times I_4$	22
$I_2^5 \times I_6$	4
I_2^6	14
$I_2^6 \times I_4$	2
I_2^7	1
I_2^8	1
I_3	93
I_3^2	2
I_3^3	4
$I_3^3 \times I_6$	4
$I_3^3 \times I_9$	2
I_3^4	6
$I_3^4 \times I_6$	4
I_3^5	2
I_4	95
I_4^4	1
I_5	12
I_6	2

Table 18: *List of generic non-toric Sp and SU-type Kodaira singularities and the number of times they occur, part II.*

References

[1] C. Vafa, *Evidence for F theory*, *Nucl.Phys.* **B469** (1996) 403–418, [hep-th/9602022].

[2] V. Braun and D. R. Morrison, *F-theory on Genus-One Fibrations*, *JHEP* **1408** (2014) 132, [arXiv:1401.7844].

[3] P. Candelas and A. Font, *Duality between the webs of heterotic and type II vacua*, *Nucl.Phys.* **B511** (1998) 295–325, [hep-th/9603170].

[4] M. Bershadsky, K. A. Intriligator, S. Kachru, D. R. Morrison, V. Sadov, *et. al.*, *Geometric singularities and enhanced gauge symmetries*, *Nucl.Phys.* **B481** (1996) 215–252, [hep-th/9605200].

[5] P. Candelas, E. Perevalov, and G. Rajesh, *Toric geometry and enhanced gauge symmetry of F theory / heterotic vacua*, *Nucl.Phys.* **B507** (1997) 445–474, [hep-th/9704097].

[6] T. W. Grimm and T. Weigand, *On Abelian Gauge Symmetries and Proton Decay in Global F-theory GUTs*, *Phys.Rev.* **D82** (2010) 086009, [arXiv:1006.0226].

[7] D. R. Morrison and D. S. Park, *F-Theory and the Mordell-Weil Group of Elliptically-Fibered Calabi-Yau Threefolds*, *JHEP* **1210** (2012) 128, [arXiv:1208.2695].

[8] V. Braun, T. W. Grimm, and J. Keitel, *New Global F-theory GUTs with U(1) symmetries*, *JHEP* **1309** (2013) 154, [arXiv:1302.1854].

[9] T. W. Grimm, A. Kapfer, and J. Keitel, *Effective action of 6D F-Theory with U(1) factors: Rational sections make Chern-Simons terms jump*, *JHEP* **1307** (2013) 115, [arXiv:1305.1929].

[10] M. Kuntzler and S. Schafer-Nameki, *Tate Trees for Elliptic Fibrations with Rank one Mordell-Weil group*, arXiv:1406.5174.

[11] J. Borchmann, C. Mayrhofer, E. Palti, and T. Weigand, *SU(5) Tops with Multiple U(1)s in F-theory*, *Nucl.Phys.* **B882** (2014) 1–69, [arXiv:1307.2902].

[12] M. Cvetic, D. Klevers, and H. Piragua, *F-Theory Compactifications with Multiple U(1)-Factors: Constructing Elliptic Fibrations with Rational Sections*, *JHEP* **1306** (2013) 067, [arXiv:1303.6970].

[13] M. Cvetič, A. Grassi, D. Klevers, and H. Piragua, *Chiral Four-Dimensional F-Theory Compactifications With SU(5) and Multiple U(1)-Factors*, *JHEP* **1404** (2014) 010, [arXiv:1306.3987].

[14] J. Borchmann, C. Mayrhofer, E. Palti, and T. Weigand, *Elliptic fibrations for $SU(5) \times U(1) \times U(1)$ F-theory vacua*, *Phys.Rev.* **D88** (2013), no. 4 046005, [arXiv:1303.5054].

[15] M. Cvetic, D. Klevers, H. Piragua, and P. Song, *Elliptic fibrations with rank three Mordell-Weil group: F-theory with U(1) x U(1) x U(1) gauge symmetry*, *JHEP* **1403** (2014) 021, [arXiv:1310.0463].

[16] V. Braun, T. W. Grimm, and J. Keitel, *Geometric Engineering in Toric F-Theory and GUTs with U(1) Gauge Factors*, *JHEP* **1312** (2013) 069, [arXiv:1306.0577].

[17] D. Klevers, D. K. M. Pena, P.-K. Oehlmann, H. Piragua, and J. Reuter, *F-Theory on all Toric Hypersurface Fibrations and its Higgs Branches*, arXiv:1408.4808.

[18] D. R. Morrison and W. Taylor, *Sections, multisections, and U(1) fields in F-theory*, arXiv:1404.1527.

[19] L. B. Anderson, I. García-Etxebarria, T. W. Grimm, and J. Keitel, *Physics of F-theory compactifications without section*, arXiv:1406.5180.

[20] I. García-Etxebarria, T. W. Grimm, and J. Keitel, *Yukawas and discrete symmetries in F-theory compactifications without section*, arXiv:1408.6448.

[21] C. Mayrhofer, E. Palti, O. Till, and T. Weigand, *Discrete Gauge Symmetries by Higgsing in four-dimensional F-Theory Compactifications*, arXiv:1408.6831.

[22] C. Mayrhofer, E. Palti, O. Till, and T. Weigand, *On Discrete Symmetries and Torsion Homology in F-Theory*, arXiv:1410.7814.

[23] T. W. Grimm, M. Kerstan, E. Palti, and T. Weigand, *Massive Abelian Gauge Symmetries and Fluxes in F-theory*, *JHEP* **1112** (2011) 004, [arXiv:1107.3842].

[24] A. P. Braun, A. Collinucci, and R. Valandro, *The fate of U(1)'s at strong coupling in F-theory*, *JHEP* **1407** (2014) 028, [arXiv:1402.4054].

[25] C. Mayrhofer, E. Palti, and T. Weigand, *U(1) symmetries in F-theory GUTs with multiple sections*, *JHEP* **1303** (2013) 098, [arXiv:1211.6742].

[26] V. Braun, *Toric Elliptic Fibrations and F-Theory Compactifications*, *JHEP* **1301** (2013) 016, [arXiv:1110.4883].

[27] P. Berglund and T. Hubsch, *On a residue representation of deformation, Koszul and chiral rings*, *Int.J.Mod.Phys.* **A10** (1995) 3381–3430, [hep-th/9411131].

[28] P. Deligne, *Courbes elliptiques: formulaire d'après j. tate*, in *Modular functions of one variable, IV (Proc. Internat. Summer School, Univ. Antwerp, Antwerp, 1972)*, vol. 476, pp. 53–73, 1975.

[29] S. Y. An, S. Y. Kim, D. C. Marshall, S. H. Marshall, W. G. McCallum, and A. R. Perlis, *Jacobians of genus one curves*, *J. Number Theory* **90** (2001) 304–315.

[30] W. Stein *et. al.*, *Sage Mathematics Software (Version 6.2)*. The Sage Development Team, 2014. http://www.sagemath.org.

[31] J. J. Duistermaat, *Discrete integrable systems. QRT maps and elliptic surfaces.* Springer Monographs in Mathematics. Berlin: Springer. xxii+627 pp., 2010.

[32] G. Salmon, *A Treatise on Conic Sections: Containing an Account of Some of the Most Important Modern Algebraic and Geometric Methods.* Chelsea Publishing Series. Chelsea Publishing Company, 1954.

[33] V. Braun and J. Keitel, *Invariants of Two Ternary Quadratics.* The Sage Development Team, 2013. http://trac.sagemath.org/17305.

[34] V. V. Batyrev, *Dual polyhedra and mirror symmetry for Calabi-Yau hypersurfaces in toric varieties*, *J.Alg.Geom.* **3** (1994) 493–545, [alg-geom/9310003].

[35] V. V. Batyrev and L. A. Borisov, *On Calabi-Yau complete intersections in toric varieties*,

alg-geom/9412017.

[36] M. Kreuzer and H. Skarke, *Classification of reflexive polyhedra in three-dimensions*, *Adv.Theor.Math.Phys.* **2** (1998) 847–864, [hep-th/9805190].

[37] M. Kreuzer and H. Skarke, *Complete classification of reflexive polyhedra in four-dimensions*, *Adv.Theor.Math.Phys.* **4** (2002) 1209–1230, [hep-th/0002240].

[38] M. Kreuzer and H. Skarke, *PALP: A Package for analyzing lattice polytopes with applications to toric geometry*, *Comput.Phys.Commun.* **157** (2004) 87–106, [math/0204356].

[39] J. H. Silverman, *The arithmetic of elliptic curves*, vol. 106. Springer, 2009.

[40] A. Novoseltsev, *Lattice polytope module for Sage*. The Sage Development Team, 2010. http://www.sagemath.org/doc/reference/geometry/sage/geometry/lattice_polytope.html.

[41] V. Braun and A. Novoseltsev, *Toric geometry module for Sage*. The Sage Development Team, 20130. http://www.sagemath.org/doc/reference/schemes/sage/schemes/toric/variety.html.

[42] W. Decker, G.-M. Greuel, G. Pfister, and H. Schönemann, "SINGULAR 3-1-6 — A computer algebra system for polynomial computations." http://www.singular.uni-kl.de, 2012.

[43] P. Candelas, A. Constantin, and H. Skarke, *An Abundance of K3 Fibrations from Polyhedra with Interchangeable Parts*, *Commun. Math. Phys.* **324** (2013) 937–959, [arXiv:1207.4792].

[44] V. Bouchard and H. Skarke, *Affine Kac-Moody algebras, CHL strings and the classification of tops*, *Adv.Theor.Math.Phys.* **7** (2003) 205–232, [hep-th/0303218].

[45] T. W. Grimm and H. Hayashi, *F-theory fluxes, Chirality and Chern-Simons theories*, *JHEP* **1203** (2012) 027, [arXiv:1111.1232].

[46] M. Cvetic, T. W. Grimm, and D. Klevers, *Anomaly Cancellation And Abelian Gauge Symmetries In F-theory*, *JHEP* **1302** (2013) 101, [arXiv:1210.6034].

[47] M. Esole, J. Fullwood, and S.-T. Yau, *D_5 elliptic fibrations: non-Kodaira fibers and new orientifold limits of F-theory*, arXiv:1110.6177.

[48] C. Mayrhofer, D. R. Morrison, O. Till, and T. Weigand, *Mordell-Weil Torsion and the Global Structure of Gauge Groups in F-theory*, *JHEP* **1410** (2014) 16, [arXiv:1405.3656].

[49] A. Grassi and D. R. Morrison, *Anomalies and the Euler characteristic of elliptic Calabi-Yau threefolds*, *Commun.Num.Theor.Phys.* **6** (2012) 51–127, [arXiv:1109.0042].

[50] C. Long, L. McAllister, and P. McGuirk, *Heavy Tails in Calabi-Yau Moduli Spaces*, *JHEP* **1410** (2014) 187, [arXiv:1407.0709].

[51] D. R. Morrison and W. Taylor, *Classifying bases for 6D F-theory models*, *Central Eur.J.Phys.* **10** (2012) 1072–1088, [arXiv:1201.1943].

[52] D. R. Morrison and W. Taylor, *Toric bases for 6D F-theory models*, *Fortsch.Phys.* **60** (2012) 1187–1216, [arXiv:1204.0283].

[53] T. W. Grimm and W. Taylor, *Structure in 6D and 4D N=1 supergravity theories from F-theory*, *JHEP* **1210** (2012) 105, [arXiv:1204.3092].

[54] G. Martini and W. Taylor, *6D F-theory models and elliptically fibered Calabi-Yau threefolds over semi-toric base surfaces*, arXiv:1404.6300.